PERIODIC OPTIMIZATION OF BIOLOGICAL SYSTEMS

By

EVA-MARIA ABULESZ

A DISSERTATION PRESENTED TO THE GRADUATE SCHOOL
OF THE UNIVERSITY OF FLORIDA IN PARTIAL FULFILLMENT
OF THE REQUIREMENTS FOR THE DEGREE OF
DOCTOR OF PHILOSOPHY

UNIVERSITY OF FLORIDA

1988

To
Emma and Alfred Hoenig

ACKNOWLEDGEMENTS

I wish to express my sincere thanks to and respect for Professor Gerasimos Lyberatos. His insight and profound knowledge as well as his patience made it easier for me to adapt to a more theoretical approach to research. I sincerely appreciate the opportunity he has given me to develop my own research interests and thus to discover the area of medical research in which I hope to continue working.

I owe thanks to the members of my Ph.D. committee for their advice and to the staff of the CAD/CAM facility, who patiently endured my complaints about not enough disc space or computer time.

I would like to thank Mark Stephens for his help.

I am grateful to Debbie Hitt for the typing of this dissertation.

I am very thankful to my parents, Eva and Karl Abulesz, and to my grandparents, Therese and Karl Abulesz, for their support and their (often needed) financial contributions.

I wish to thank my sister, Christa Habla, who being so very different from myself, often helped me to focus on the really important things in life.

And, of course, many thanks are due to my good friends who, over the years, helped me preserve my mental sanity, especially to Yvette, Cheryl and Greg, and Lyn.

TABLE OF CONTENTS

Abstract of Dissertation Presented to the Graduate School
of the University of Florida in Partial Fulfillment of the
Requirements for the Degree of Doctor of Philosophy

PERIODIC OPTIMIZATION OF BIOLOGICAL SYSTEMS

by

Eva-Maria Abulesz

August 1988

Chairman: Dr. Hong H. Lee
Major Department: Chemical Engineering

In bioprocessing and medicine periodic conditions frequently prove to be more successful in achieving a certain objective than steady-state conditions. Often this is due to the fact that cells need some time to adapt to new conditions, when their environment changes. If one can use this lag-time to aid in reaching the goal of interest, periodic operating conditions are highly desirable.

In this dissertation methods of optimal control theory are applied to establish the optimal periodic conditions in two major areas: fermentation technology and cancer chemotherapy.

The method of π-criterion is used to determine whether periodic variation of the dilution rate can enhance the performance of continuous fermentation processes. It is found that the presence of a time-delay in the dynamic response of the chemostat renders a periodic operation of bioreactors which results in enhanced biomass productivity. Also employing Williams's structured model it is shown that cycling can improve the average protein productivity.

Experiments with S. cerevisiae are described which aim at verifying these predictions. The dynamic model found to describe step changes in dilution rate incorporates a lag-time during which the culture adapts to the new environmental conditions. It was confirmed that for certain cycling frequencies periodic reactor operation results in enhanced biomass productivity.

The π-criterion is then applied to cancer chemotherapy. A procedure is proposed which allows to determine the optimal treatment regimen given a certain patient and drug. As a result it can be seen whether the drug under consideration will have the desired effect as well as which form of treatment would be preferable: cycling (on/off) or continuous. In the event cyclic treatment is superior, the optimal treatment regimen is established.

To assess the effect a series of injections of drug has on the normal and malignant cell population, and on the performance measure, a new method, "periodic impulse forcing of nonlinear systems," is developed. The method is based on the Carleman linearization procedure and allows the determination of the state equations and the performance measure as a function of the forcing period. It is subsequently applied to a model for cancer chemotherapy.

CHAPTER I
GENERAL INTRODUCTION

Motivation and Background

In the area of biochemical engineering, although substantial research effort has been invested in the optimization of batch and semi-batch processes [1-6], very little has been done in the optimization of continuous bioreactors [7]. Over the past few years it has been realized that steady-state operation of chemical reactors is not necessarily the optimum type of operation. If some manipulated process variables are allowed to vary with time, very often superior productivity, parametric insensitivity or even a change of the culture fate is possible when compared to steady-state operation. A significant amount of work has been undertaken [8-14] to establish the periodic operations that maximize the yields and/or selectivities of chemical reactors. Some workers [15-20] have tried to assess the effect of cycling behavior of a chemostat culture experimentally, but it is hard to draw any general conclusions since frequently undefined growth media (e.g., molasses) or insufficiently defined quantities were used.

The quality of any optimization depends to a great extent on how well the mathematical model at hand describes the process in question. In general two types of models are used to describe microbial growth processes: "unstructured models" and "structured models." Unstructured models have inherent the assumption of balanced growth. This indicates that every single part of the cell grows at the same rate during a period of balanced growth. This situation may be viewed as the state

reached after all the transients have died out and the cell has adapted to a constant environment, essentially at steady-state. For this very reason unstructured models succeed in describing steady-state situations, but they are in general insufficient in accurately portraying dynamic systems. For such systems the assumption of balanced growth has to be relaxed. This can be done in two ways. The first possibility is to include a time-delay in the mathematical description of the system. Introducing a time-delay increases the dimensionality of the mathematical model but it allows a better description of dynamic situations. Moreover it is also physiologically meaningful because it essentially assumes that the cell does not react to a change in environmental conditions by an instantaneous adaptation of its growth rate.

The alternate way to relax the assumption of balanced growth is the formulation of a structured model. Such models break down the cell in separate compartments, as many as needed, but at least two, and allow for each compartment to grow at its own rate. Structured models are superior to unstructured ones in describing dynamic situations. It is not very meaningful, though, to use models of too high dimensionality because aside from their mathematical complexity, many of the state variables in such models (nucleic acids, metabolites, growth factors) are not readily measurable, especially on line, something that makes the determination of system parameters practically impossible.

Based on these various types of mathematical models methods, of optimal control theory will be used to detect the desirability of periodic reactor operation. Moreover, if periodic operation is the operation of choice, an estimate of the optimal cycling frequency will be obtained. Experiments will be conducted to assess the effect of cyclic reactor operation on yeast in a chemostat culture.

Just as the growth of micro-organisms can be stimulated by a certain "feeding schedule," the growth of tumor cells can be minimized by a certain "treatment schedule." Unfortunately the situation here is much more complex than in the case of uni-cellular organisms. So far the success of chemotherapy and radiation therapy has been limited. Surgery proves ineffective in about half of all cases because the tumor was discovered too late and metastases have already spread throughout the body. So it is not surprising that up to 400,000 people die from cancer every year in the U.S. alone.

Healthy mammalian cells are under strict homeostatic control. New cell formation is turned on or off according to the body's need. In cancer cells, however, the control mechanism breaks down and uncontrolled growth occurs. Therefore a cancer cell has a selective advantage over a benign, controlled cell. Cancer cells in general do not grow faster than normal body cells. Cancer cells found even in constantly proliferating tissues like epithelium or bone marrow have longer cell-cycle times than their benign stem cell. What makes cancer such a dreadful disease and its treatment extremely difficult is its invasiveness of other body compartments, making localized surgery ineffective. Recent alternatives like monoclonal antibodies are still in their infant stages and so chemotherapy, though not an optimal form of treatment, has to be improved in any way possible. The approach followed in this dissertation is based on the mathematical modeling of normal and cancer cells. The kinetic differences between those cell types are used to optimize the treatment schedule. Recall that unstructured models in general fail to predict the dynamic of even a unicellular organism. That is even more so for such a complex structure

as the human body. Because it is not an ideal CSTR (continuous stirred tank reactor) with complete mixing it is frequently necessary to introduce models comparable to the structured models introduced above. In pharmacokinetic modeling the body is, if needed, divided into various compartments each exhibiting similar kinetic properties. These compartments may or may not comprise physical entities, such as organs. But, of course, the model should be kept as simple as possible, describing all the known facts and able to support the intended purpose. For this reason this work is limited to one-compartment pharmacokinetic models and cycle non-specific drugs as a first stepping stone towards predictable chemotherapy.

Dissertation Outline

In this dissertation, biological processes like continuous fermentations and drug therapy will be described by a mathematical model. Using two methods of periodic optimal control, the optimal periodic input (or the optimal steady state operation, if it is found to be superior) is determined. Experiments are described which assess how periodic input actually influences the chemostat culture.

In Chapter II the optimization theory used in this thesis will be presented. Following an overview of relevant optimal control theory and the π-criterion (II.1.) a new method will be introduced (II.2.), concerned with periodic impulse forcing of nonlinear systems. It allows the explicit evaluation of the performance measure of such a system as a function of the cycling frequency.

Chapter III deals with the application of periodic optimal control to continuous fermentations. In the first part (III.1) the desirability

of periodic operation is evaluated for unstructured models, unstructured models with time-delay and structured models. In the second part (III.2.) experimental results on the behavior of Saccharomyces cerevisiae (yeast) in a chemostat culture under periodic square wave forcing are presented.

In Chapter IV, optimal control theory is applied to cancer chemotherapy. In the first part of this chapter (IV.1.) it is shown how one can determine whether periodic or continuous treatment of cancer renders better results and how appropriate the drug(s) used is (are) in a particular situation.

The new method described in Section II.2. will be applied to drug therapy in Section (IV.2.) to assess the effect of repeated injections (periodic impulse forcing).

Chapter V finally draws general conclusions obtained from this study of periodic optimization of biological systems.

CHAPTER II
METHODS OF OPTIMAL CONTROL THEORY
AND PERIODIC OPTIMIZATION

II. 1. Optimal Control Theory and the π-Criterion: An Overview

Introduction

To apply optimal control theory to an optimization problem requires the following:

- a mathematical model of the process to be controlled
- the knowledge of all constraints
- a known objective, the performance criterion

The classical control problem is the one where an object shall be moved from a state A to a state B. The object might be a car, a rocket or the vector of state variables for a chemical reaction; the states might be points in space or the steady states of a reaction system.

The state of the car, for example, can be described by its position and its velocity (state variables). It can be controlled by varying the acceleration and the brake deceleration (control variables) of the vehicle. The task to perform can be to move the car from point A to point B on a straight line. Its motion can be described by the equations of classical mechanics (mathematical model of the process).

In general three kinds of constraints can be distinguished: state constraints, which define the values of the state variables at points in space and time--often called "boundary conditions" (e.g. at the initial and the final time the car is stationary); control constraints, which

set limits on the admissible values for the control variables (e.g. the highest possible acceleration is ...); and additional constraints (e.g. the amount of gas in the tank).

Knowing the model, the constraints and the task to be performed, the question arises what is the "best," the "optimal" way to perform this task? What are the criteria, that make one trajectory (history of state variables) better than the other? If the objective is to move the car from A to B in the least amount of time, then the fastest admissible trajectory is better than any slower one. If the objective is to use the least amount of gas on the way, then a slower trajectory might be optimal. The objective is reflected in the "performance measure" or the "performance criterion."

In the same way as this problem of classical mechanics can be solved, biological systems can be optimized. Whether the objective is the fastest growth of a microorganism, the highest productivity of an antibiotic or the maximum kill of tumor cells, the principles stated above are still valid.

In the next section the optimization problem will be formulated mathematically.

Mathematical Formulation of the Optimization Problem

Let the process to be optimized be defined by a set of ordinary differential equations (although other descriptions such as partial differential equations are also allowable), which adequately describes the response of the system to all possible inputs. Assuming that $\underline{f}$ has continuous partial derivatives in $\underline{x}$ and $\underline{u}$,

$$\dot{\underline{x}}(t) = \underline{f}\ (\underline{x}(t),\ \underline{u}(t),\ t) \tag{2-1}$$

where

$$x(t) = \begin{vmatrix} x_1(t) \\ x_2(t) \\ . \\ . \\ x_r(t) \end{vmatrix} \tag{2-2}$$

is the vector of state variables or state vector and

$$u(t) = \begin{vmatrix} u_1(t) \\ u_1(t) \\ . \\ . \\ u_s(t) \end{vmatrix} \tag{2-3}$$

is the vector of control variables or control vector.

In most cases the objective of the process can be fulfilled by a multitude of different control vectors, called the admissible controls. The purpose of applying optimal control theory is to determine the admissible control which maximizes or minimizes the performance criterion J which is given by

$$J = \int_{t_o}^{t_f} \phi\ (\underline{x}(t),\ \underline{u}(t),\ t)dt + \psi\ (\underline{x}(t_f),\ t_f) \tag{2-4}$$

where t_o and t_f are the initial and the final time, respectively, and ϕ and ψ are scalar functions, possessing continuous partial derivations in $\underline{x}$ and $\underline{u}$. The first term in equation (2-4) depends on the state trajectory, which in turn is determined by the control history and the

initial conditions, over the time interval $\Delta t = t_f - t_o$, whereas the second term is a function of the final state only.

The Pontryagin Maximum Principle

An optimal control $\underline{u}_{opt}$ maximizes the performance criterion J if

$$\Delta J = J(\underline{u}_{opt}) - J(\underline{u}) \geq 0 \tag{2-5}$$

Any control $\underline{u}$ (if sufficiently close to $\underline{u}_{opt}$) can be expressed as

$$\underline{u} = \underline{u}_{opt} + \delta\underline{u} \tag{2-6}$$

so that the necessary condition to minimize the functional J becomes

$$\delta J(\underline{u}_{opt}, \delta\underline{u}) \geq 0 \tag{2-7a}$$

if $\underline{u}_{opt}$ lies on the boundary of admissible values for the control $\underline{u}$ at any time during the interval Δt, or

$$\delta J(\underline{u}_{opt}, \delta\underline{u}) = 0 \tag{2-7b}$$

if $\underline{u}_{opt}$ lies within the boundaries in the time interval Δt.

Recall now the functional to minimize as given by equation (2-4). Rewriting the performance measure as

$$J = \int_{t_o}^{t_f} [\phi(\underline{x}(t), \underline{u}(t), t) + \underline{\lambda}^T(t)\underline{f}(\underline{x}(t), \underline{u}(t), t) - \dot{\underline{x}}(t)] - \psi(\underline{x}(t_f), t_f) \tag{2-8}$$

where $\underline{\lambda}$ is the vector of adjoint variables or Lagrange Multipliers, and defining the Hamiltonian

$$H(\underline{x}(t), \underline{u}(t), \underline{\lambda}(t), t) = \phi(\underline{x}(t), \underline{u}(t), t) + \underline{\lambda}^T(t)\underline{f}(\underline{x}(t), \underline{u}(t), t) \tag{2-9}$$

it is obvious that

$$J = \int_{t_o}^{t_f} [H(\underline{x}(t), \underline{u}(t), t) - \underline{\lambda}^T(t)\dot{\underline{x}}(t)]dt + \psi(\underline{x}(t_f), t_f) \tag{2-10}$$

which can be integrated by part to yield

$$J = \int_{t_o}^{t_f} [H(\underline{x}(t), \underline{u}(t), t) + \dot{\underline{\lambda}}^T\underline{x}(t)]dt + \psi(\underline{x}(t_f), t_f) - \underline{\lambda}^T\underline{x}\Big|_{t_o}^{t_f} \tag{2-11}$$

It can be shown [21] that to minimize J it is necessary that

$$H(\underline{x}_{opt}(t), \underline{u}_{opt}(t) + \delta\underline{u}(t), \underline{\lambda}_{opt}(t), t) \geq H(\underline{x}_{opt}(t), \underline{u}_{opt}(t), \underline{\lambda}_{opt}(t), t) \tag{2-12}$$

Equation (2-12) is the essence of the Pontryagin Minimum Principle. It states that to maximize the performance criterion J an optimal control $\underline{u}_{opt}$ has to maximize the Hamiltonian H.

Summarizing, for a process described by equations (2-1) - (2-3) and a performance measure as given by equation (2-4) to be optimized by an optimal control vector $\underline{u}_{opt}$, the Hamiltonian is defined as in equation (2-9). The following conditions must hold for $t \in \Delta t$:

$$\frac{\partial H}{\partial \underline{u}} = 0 \tag{2-13}$$

$$\dot{\underline{x}} = \frac{\partial H}{\partial \underline{\lambda}} \tag{2-14}$$

$$\dot{\underline{\lambda}} = -\frac{\partial H}{\partial \underline{x}} \tag{2-15}$$

Equations (2-13) - (2-15) define a system of equations in $\underline{x}$ and $\underline{\lambda}$. A two-point boundary problem has to be solved. The boundary conditions are provided by the transversality conditions

$$\partial \underline{x}^T \left(\frac{\partial \psi}{\partial \underline{x}} - \underline{\lambda} \right) = 0 \tag{2-16}$$

for $t = t_o$ and t_f.

The π-criterion

As discussed in Chapter 1 in many cases periodic operation proves to be very desirable. The problem of determining the optimum periodic operation was addressed by Bittanti et al. [22] who developed the so called π-criterion for optimality. This criterion states a sufficient condition for improvement of the performance of a periodic system via cycling. The method in addition provides an estimate of the optimum cycling frequency for the particular system of interest.

This section sets the mathematical framework for studying periodic optimization problems by applying the π-criterion.

Recall the model equations as given by equation (2-1) and let

$$\underline{y}(t) = \underline{h}(\underline{x}(t), t) \tag{2-17}$$

be the equation relating the measured variables $\underline{y}$ to the state variables $\underline{x}$. Assume that there exists a steady-state solution corresponding to $\underline{u} = \underline{u}^o$ for which $\underline{x} = \underline{x}^o$ and $\underline{y} = \underline{y}^o$, at which a performance measure $J = \phi(\underline{u}, \underline{y})$ is maximized. We seek a periodic operation of the form

$$\underline{u}(t) = \underline{u}(t + \tau) \tag{2-18}$$

that would lead to an average performance measure

$$J(\underline{u}(\cdot); \tau) = \frac{1}{\tau} \int_o^\tau \phi(\underline{u}, \underline{y})dt \tag{2-19}$$

which is higher than $J^o = J_{opt} = \phi(\underline{u}_{opt}, \underline{y}_{opt})$.

In most cases it is a good assumption [23] that a control policy of the form (2-18) leads to a periodic solution of the same period; i.e.

$$\underline{x}(t + \tau) = \underline{x}(t) \tag{2-20}$$

The optimization is in general subject to equality constraints of the form

$$\frac{1}{\tau} \int_o^\tau \underline{v}(\underline{y}, \underline{u})dt = 0 \tag{2-21}$$

and inequality constraints of the form

$$\frac{1}{\tau}\int_0^\tau \underline{w}(\underline{y},\underline{u})dt \leq 0 \tag{2-22}$$

Assuming that $\underline{f}(\underline{x},\underline{u})$, $\underline{h}(\underline{x})$, $\phi(\underline{y},\underline{u})$, $\underline{v}(\underline{y},\underline{u})$ and $\underline{w}(\underline{y},\underline{u})$ are twice differentiable at the optimum steady-state, one can define the Hamiltonian

$$H(\underline{x},\underline{u},\underline{\lambda},\underline{\mu}) \equiv \phi(\underline{h}(\underline{x}), \underline{u}) + \underline{\lambda}^T\underline{f}(\underline{x}, \underline{u}) + \underline{\mu}^T\underline{v}(\underline{h}(\underline{x}), \underline{u}) \tag{2-23}$$

$\underline{\lambda}$ and $\underline{\mu}$ being Lagrange multipliers.

Let

$$\pi(\omega) = G^*(-j\omega)PG(j\omega) + Q^*G(j\omega) + G^*(-j\omega)Q + R \tag{2-24}$$

where

$$G(p) = (pI - A)^{-1}B \tag{2-25}$$

and

$$A = \underline{f}_{\underline{x}}(\underline{x}^o, \underline{u}^o) \tag{2-26}$$

$$B = \underline{f}_{\underline{u}}(\underline{x}^o, \underline{u}^o) \tag{2-27}$$

$$P = H_{\underline{x}\underline{x}}(\underline{x}^o, \underline{u}^o, \underline{\lambda}^o, \underline{\mu}^o) \tag{2-28}$$

$$Q = H_{\underline{x}\underline{u}}(\underline{x}^o, \underline{u}^o, \underline{\lambda}^o, \underline{\mu}^o) \tag{2-29}$$

$$R = H_{\underline{\underline{uu}}}(\underline{x}^o, \underline{u}^o, \underline{\lambda}^o, \underline{\mu}^o) \tag{2-30}$$

Then the π-criterion states that if the (n x n) Hermitian matrix $\pi(\omega)$ is partially positive for some values of $\omega > 0$, then there exist $\omega > 0$ such that $\pi(\omega)$ is not negative definite [22]. For single input-single output systems of the type concerned with this work, $\pi(\omega)$ is simply a scalar function of the frequency ω. For the optimization problems of interest it then suffices to have $\pi > 0$ for some cycling frequencies ω. This will guarantee that operating at such cycling frequencies will result in superior bioreactor performance.

II. 2. Periodic Impulse Forcing of Nonlinear Systems-- A New Method

Introduction

The π-criterion, as introduced in Section (II.1.), gives only sufficient conditions for the improvement of the performance of a certain system by periodic operation. Moreover, it is strictly valid only locally and does not give any information about the optimal wave form or amplitude. To obtain this information, tedious and time consuming integrations have to be performed. A new procedure is needed to obtain a direct relationship between the performance criterion, the forcing frequency and the system parameters.

In the practice of periodic operation the two most easily implementable wave forms are impulse- and pulse-forcing. For the case of pulse forcing, Lyberatos and Svoronos [24] utilized the Carleman linearization procedure to develop a method which allows the determination of the

performance measure as a function of the three pulse forcing parameters, which suffice to describe the system. Their result is given in Appendix A.

Impulse-forcing has widespread applications in many areas of industry, biology and medicine. Semibatch-operation of a reactor, periodic harvesting of a fishculture in a pond, repeated injections of antibiotics into a fermentor or periodic injections of drugs in medicine are just a few examples. Since this method is easily implementable, often more economical and in many cases improves the performance of the system, it frequently proves to be the operation of choice.

The mathematical characterization of this type of operation, on the other hand, often proves to be rather difficult or impossible. If the mathematical model employed is linear, the evaluation of the time-dependence of the state variables is straightforward. For nonlinear models, so far only numerical methods have generally been used.

In the following, the Carleman linearization procedure is applied to evaluate systems which undergo periodic impulse forcing. This new method is applicable to nonlinear lumped parameter systems and performance measures and it allows the explicit evaluation of the time-dependence of the system as well as the performance measure.

The next section states the mathematical problem, followed by a review of the Carleman linearization procedure. Then the new method is introduced and illustrated by an example.

Statement of the Problem

Consider the nonlinear system

$$\dot{\underline{y}} = \underline{f}(\underline{y}) \tag{2-31}$$

with

$$f(\underline{o}) = \underline{o} \tag{2-32}$$

Suppose a series of impulses is introduced with a period τ which results in an instantaneous addition of a disturbance $\underline{m}$ to the state vector $\underline{y}$. Assuming that the response is also τ-periodic, after all transients have died out, the following relationship must hold,

$$\underline{y}_f = \underline{y}_o - \underline{m} \tag{2-33}$$

where $\underline{y}_o$ and $\underline{y}_f$ denote the values of the state variables at the beginning and end of the period respectively. The objective of this investigation is to find an analytical solution for the nonlinear system as described by equations (2-31) and (2-32) which makes it possible to calculate explicitly an average performance measure J which can be written as

$$J = \frac{1}{\tau} \int_o^\tau P(\underline{y})\, dt \tag{2-34}$$

as a function of the forcing frequency.

The Carleman Linearization Procedure

The Carleman linearization procedure is an approximation of a nonlinear system by a linear system of higher order [25]. Its previous application to nonlinear system dynamics and control can be found in references 26-35. The procedure will be outlined in the following.

The function $\underline{f}$ of system (2-31), assuming it is differentiable up to order ℓ at $\underline{y} = \underline{0}$, is expanded into a Taylor-series and the monomials of order up to ℓ are introduced as new variables. When these monomials are differentiated and only terms up to order ℓ are retained, a higher order linear system in the new variables is obtained. For example the system

$$\dot{x}_1 = (\sin x_1)x_2 \tag{2-35a}$$

$$\dot{x}_2 = x_2 + x_1x_2 \tag{2-35b}$$

is Taylor-expanded around zero into

$$\dot{x}_1 = x_1x_2 + O(x^3) \tag{2-36a}$$

$$\dot{x}_2 = x_2 + x_1x_2 \tag{2-36b}$$

This system has the second order Carleman linearization:

$$\underline{\dot{w}} = \frac{d}{dt}\begin{pmatrix} x_1 \\ x_2 \\ x_1^2 \\ x_1x_2 \\ x_2x_1 \\ x_2^2 \end{pmatrix} = \begin{pmatrix} 0 & 0 & 0 & 1 & 0 & 0 \\ 0 & 1 & 0 & 1 & 0 & 0 \\ 0 & 0 & 0 & 0 & 0 & 0 \\ 0 & 0 & 0 & 1 & 0 & 0 \\ 0 & 0 & 0 & 0 & 1 & 0 \\ 0 & 0 & 0 & 0 & 0 & 2 \end{pmatrix} \underline{w} \qquad (2\text{-}37)$$

In general the Taylor series approximation of system (2-31) around $\underline{y} = \underline{o}$ can be written as

$$\dot{\underline{y}} = \sum_{j=1}^{\infty} A_{1,j}\, \underline{y}^{[j]} \qquad (2\text{-}38)$$

where $\underline{y}^{[j]} = \underline{y} \times \underline{y} \times \ldots \times \underline{y}$ ($\times$ denotes Kronecker multiplication).

The ℓth order Carleman linearization is the approximation of the original system by the following linear system:

$$\underline{\dot{w}} = \begin{pmatrix} \dot{\underline{y}} \\ \dot{\underline{y}}^{[2]} \\ \cdot \\ \cdot \\ \cdot \\ \cdot \\ \cdot \\ \dot{\underline{y}}^{[\ell]} \end{pmatrix} = \begin{pmatrix} A_{1,1} & A_{1,2} & \cdot & \cdot & \cdot & \cdot & A_{1,\ell} \\ 0 & A_{2,1} & \cdot & \cdot & \cdot & \cdot & A_{2,\ell-1} \\ \cdot & & & & & & \\ \cdot & \cdot & & & & & \\ \cdot & & \cdot & & & & \\ \cdot & & & \cdot & & & \\ \cdot & & & & \cdot & & \\ 0 & \cdot & \cdot & \cdot & \cdot & \cdot & A_{\ell,1} \end{pmatrix} \underline{w} \qquad (2\text{-}39)$$

where

$$A_{i,j} = A_{1,j} \otimes I_{n^{i-1}} + I_n \otimes A_{i-1,j} \qquad (2\text{-}40)$$

Solving Nonlinear Systems Undergoing Impulse Forcing by Using the Carleman Linearization Procedure

As outlined in the previous section, the nonlinear system described by equation (2-31) can be approximated through the Carleman linearization procedure to yield the following linear system

$$\dot{\underline{w}} = C_{\ell}\underline{w} \tag{2-41}$$

where C_{ℓ} is the ℓth order Carleman matrix and is given by

$$C_{\ell} = \begin{pmatrix} A_{1,1} & A_{1,2} & \cdot & \cdot & \cdot & \cdot & A_{1,\ell} \\ 0 & A_{2,1} & \cdot & \cdot & \cdot & \cdot & A_{2,\ell-1} \\ \cdot & & & & & & \\ \cdot & & & & & & \\ \cdot & & & & & & \\ \cdot & & & & & & \\ 0 & 0 & \cdot & \cdot & \cdot & \cdot & A_{\ell,1} \end{pmatrix} \tag{2-42}$$

where $A_{i,j}$ is given by equation (2-40). This linear system has the solution

$$\underline{w}_f = e^{C_{\ell}\tau}\underline{w}_o \tag{2-43}$$

where $\underline{w}_f$ and $\underline{w}_o$ are the vectors of Carleman variables at the final and initial time, respectively, and τ denotes the period. In any τ-periodic system the value of $\underline{w}_f$ is given by

$$\underline{w}_f = \left[(\underline{w}_o - \underline{m}) \quad (\underline{w}_o - \underline{m})^{[2]} \ \ldots \ (\underline{w}_o - \underline{m})^{[\ell]} \right]^T \tag{2-44}$$

where $\underline{m}$ is the impulse vector.

In a similar manner the function P in the performance-measure (equation (2-34)) can be expanded into a Taylor series around $\underline{0}$ so that the performance-measure takes the following form in Carleman coordinates:

$$J = \frac{1}{\tau}\int_0^{\tau} \underline{r}^T \underline{w}(t)\, dt = \frac{\underline{r}^T}{\tau} C_{\ell}^{-1} \left[e^{C_{\ell}\tau} - I\right] \underline{w}_o \tag{2-45}$$

Theorem. The vector of state variables at the beginning of a period, $\underline{w}_o$ is given by

$$\underline{w}_o = \left[e^{C_{\ell}\tau} - \sum_{i=0}^{\ell-1} A_i\right]^{-1} \underline{m}^* \tag{2-46}$$

where

$$\underline{m}^* = \begin{pmatrix} (-\underline{m}) \\ (-\underline{m})^{[2]} \\ \cdot \\ \cdot \\ \cdot \\ (-\underline{m})^{[\ell]} \end{pmatrix} \tag{2-47}$$

$$A_o = I \tag{2-48}$$

and for $i \geq 1$

$$A_i = \begin{pmatrix} \underline{0}_{n \times n} & \cdots & \cdots & \cdots & \underline{0}_{n \times n^{\ell}} \\ \vdots & & & & \vdots \\ \underline{0}_{n^i \times n} & & & & \\ \Sigma^* I \times (-\underline{m})^{[i]} & \ddots & & & \\ \vdots & \ddots & \ddots & & \vdots \\ \underline{0}_{n^{\ell} \times n} & \cdots & \Sigma^* I^{[\ell-i]} \times (-\underline{m})^{[i]} & \underline{0}_{n^{\ell} \times n^{\ell-i+1}} & \underline{0}_{n^{\ell} \times n^{\ell}} \end{pmatrix} \qquad (2\text{-}49)$$

A general example is given in Appendix B. Here the symbol Σ^* denotes "sum of all possible orderings;" for example

$$\Sigma^*[a^3b] = a^3b + a^2ba + aba^2 + ba^3 \qquad (2\text{-}50)$$

Proof. Substituting equation (2-33) into equation (2-43) gives

$$\begin{pmatrix} (\underline{y}_o - \underline{m}) \\ (\underline{y}_o - \underline{m})^{[2]} \\ \vdots \\ (\underline{y}_o - \underline{m})^{[\ell]} \end{pmatrix} = e^{C_{\ell} T} \begin{pmatrix} \underline{y}_o \\ \underline{y}_o^{[2]} \\ \vdots \\ \underline{y}_o^{[\ell]} \end{pmatrix} \qquad (2\text{-}51)$$

where $(\underline{y}_o - \underline{m})^{[\ell]} = (\underline{y}_o - \underline{m}) \times (\underline{y}_o - \underline{m}) \times \ldots \times (\underline{y}_o - \underline{m})$

Expanding the left-hand-side of equation (2-51)

$$\begin{vmatrix} \underline{y}_o & & & + (-\underline{m}) \\ \underline{y}_o^{[2]} + \Sigma^*[Ix(-m)]\ \underline{y}_o & & & + (-\underline{m})^{[2]} \\ \vdots & & & \\ \underline{y}_o^{[\ell]} + \Sigma^*[I^{[\ell-1]}x(-m)]^{[\ell-1]}\ \underline{y}_o^{[\ell-1]} & + \ldots + & \Sigma^*[Ix(-m)^{[\ell-1]}]\underline{y}_o & + (-\underline{m})^{[\ell]} \end{vmatrix}$$

$$= e^{C_\ell \tau}\ \underline{w}_o \qquad (2\text{-}52)$$

If one defines the matrices A_i as in equations (2-48) and (2-49) and substitutes into (2-52), one obtains

$$A_0 \begin{pmatrix} \underline{y}_o \\ \underline{y}_o^{[2]} \\ \vdots \\ \underline{y}_o^{[\ell]} \end{pmatrix} + A_1 \begin{pmatrix} \underline{y}_o \\ \underline{y}_o^{[2]} \\ \vdots \\ \underline{y}_o^{[\ell]} \end{pmatrix} + A_2 \begin{pmatrix} \underline{y}_o \\ \underline{y}_o^{[2]} \\ \vdots \\ \underline{y}_o^{[\ell]} \end{pmatrix} + A_3 \begin{pmatrix} \underline{y}_o \\ \underline{y}_o^{[2]} \\ \vdots \\ \underline{y}_o^{[\ell]} \end{pmatrix} +$$

$$+ \ldots + A_{\ell-2} \begin{pmatrix} \underline{y}_o \\ \underline{y}_o^{[2]} \\ \vdots \\ \underline{y}_{-o}^{[\ell]} \end{pmatrix} + \begin{pmatrix} (-\underline{m}) \\ (-\underline{m})^{[2]} \\ \vdots \\ (-\underline{m})^{[\ell]} \end{pmatrix} = e^{C_\ell \tau} \begin{pmatrix} \underline{y}_o \\ \underline{y}_o^{[2]} \\ \vdots \\ \underline{y}_{-o}^{[\ell]} \end{pmatrix} \qquad (2\text{-}53)$$

Recognizing the vector $\underline{w}_o$ as a common multiplier and using equation (2-47), equation (2-53) becomes

$$A_0 \underline{w}_0 + A_1 \underline{w}_0 + A_2 \underline{w}_0 + A_3 \underline{w}_0 + A_{\ell-1} \underline{w}_0 + \underline{m}^* = e^{C_\ell \tau} \underline{w}_0 \qquad (2\text{-}54)$$

which can be solved for $\underline{w}_0$ to yield equation (2-46).

Remark 1. For most systems it is a good assumption [22] that inflicting disturbances periodically lead to a periodic solution of the same period; i.e.

$$\underline{y}(t + \tau) = \underline{y}(t) \qquad (2\text{-}55)$$

But as the following example shows, there can be systems or ranges of admissible periods for which this assumption is not valid. Possible outcomes include multiperiodicity or chaotic oscillations [36]. For these systems the new procedure fails to predict the occurrance of multiperiodic or random oscillations.

Remark 2. For small values of the period τ the matrix to premultiply $\underline{m}^*$ in equation (2-46) can become nearly singular. Because this matrix needs to be inverted, numerical problems might result. In that case maximum pivot-strategy (see Appendix C) should be employed.

Example

Consider the population growth-model due to Verhulst [37]

$$\dot{x} = x - x^2 \qquad (2\text{-}56)$$

and assume that harvest takes place at a constant rate of $\dot{r} = \frac{u}{\tau} = 3/16$. The average performance-measure is given by

$$J = \frac{1}{\tau} \int_0^\tau x(t)\, dt \qquad (2\text{-}57)$$

and the stable steady state is

$$\bar{x} = 3/4 \tag{2-58a}$$

at which

$$\bar{J} = 3/4 \tag{2-58b}$$

The steady-state operation shall be compared to periodic operation where at each time-interval τ a part of the population equal to $3/16\ \tau$ will be harvested. Clearly in this case $m = -\frac{3}{16}\tau$.

A major concern of the method presented is the order of the Carleman approximation that needs to be used. This is dependent on the magnitude of the disturbance, which is proportional to τ, the harvesting period. The longer the period, the larger is the disturbance, the higher is the order of approximation needed.

The system described by equation (2-56) can be solved analytically for x to yield

$$x = \frac{x_o e^{-t}}{1 + x_o(1-e^{-t})} \tag{2-59}$$

As mentioned in the previous chapter, it is of importance to know, whether the system actually is τ-periodic. A quick method to check is the procedure of "Poincare mapping," where $x_{o,n+1}$ is plotted vs. $x_{o,n}$. Figure 2-1 shows that the Verhulst-model (α=1) has three regions of τ

which exhibit different behavior. For $m = -3/16\tau$ τ-periodicity is predicted for $0 < \tau < \sim 4.1$ and $\tau > 6$. For $4.1 < \tau < 6$ random oscillations take place. This can be verified by letting $x = x_{o,n+1}$ and $t = \tau$ in equation (2-59). Solving for $x_{o,n+1}$ imaginary solutions appear in the range mentioned above. The Carleman approximation method fails to predict the region of τ where random oscillations occur. Figure 2-2 compares the exact solution to the solutions obtained by the proposed new method over one period after the transients have died out. For small values of the period τ near-singularity of the matrix to be inverted occurred, so numerical solution with maximum pivot-strategy was employed (see Appendix C). Figure 2-2 clearly shows that the approximation to the exact solution by the new method is excellent. Using a third order Carleman approximation is superior to second order as expected. Table 2-1 shows the results for the first three orders of approximation. Figure 2-3 shows how the performance measure J varies with the period τ. The agreement between the exact solution (equation (2-59)) and the approximations is good for small values of the period τ and becomes worse when τ approaches the region of chaotic oscillations. This is to be expected because the approximations fail to predict the existence of these. Agreement is achieved again for values of τ beyond the region of chaotic oscillations.

The other important result that can be seen in Figure 2-3 is that the performance measure declines with increasing period τ. This predicts that steady-state operation (continuous harvesting) is superior to periodic harvesting. If continuous harvesting is not possible, the time intervals between harvests should be kept as short as possible.

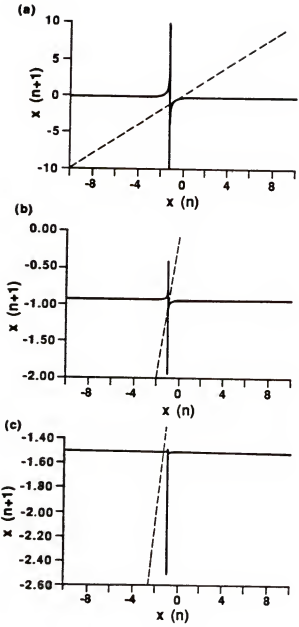

Figure (2-1). Poincare Mapping Procedure for the Verhulst model (α=1) a) τ=2, b) τ=5, c) τ=8. As τ increases, the y=x-line shifts relatively to the left. For τ=2 and τ=8 the absolute value of the slope at the point of intersection is less than 1, thus guaranteeing a stable τ-periodic solution. For τ=5 it is greater than 1, so no convergence can occur [36].

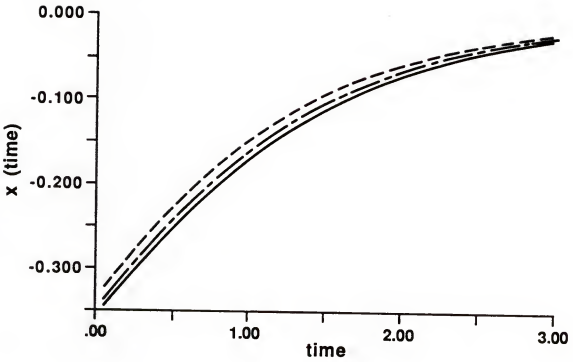

Figure (2-2). Effect of the order of the Carleman approximation. After all the transients have died out, the population x is plotted versus time for one period. The exact solution (___) is compared to the second (---) and third (.-.-) order approximation (τ=1).

Table 2-1. Results for the State Vector w_o and the Performance Measured for the First Three Orders of Approximation

1st order	$x_{o,1} = x_o = m - m(e^{-\tau}-1)^{-1}$ $J_1 = \frac{1}{\tau}\{(1 - e^{-\tau})\} x_{o,1}$
2nd order	$x_{o,1} = x_o = \frac{-me^{-2\tau} + m}{B_1(e^{-\tau} - 1)} - \frac{m^2e^{-\tau}}{B_1}$ $x_{o,2} = x_o^{[2]} = \frac{2m^2}{B_1(e^{-\tau} - 1)} + \frac{m^2}{B_1}$ $J_2 = \frac{1}{\tau}\{(1-e^{-\tau})x_{o,1} + (e^{-\tau} - \frac{e^{-2\tau}}{2} - \frac{1}{2})x_{o,2}\}$
3rd order	$x_{o,1} = x_o = \frac{-mB_3e^{-2\tau} + mB_3 + 3m^3B_4(e^{-2\tau} + 1)}{B_1B_3(e^{-\tau} - 1)} +$ $+ \frac{- B_3m^2e^{-\tau} + 3m^3B_4(me^{-\tau} + 1)}{B_1B_3} + \frac{B_4m^3}{B_3}$ $x_{o,2} = x_o^{[2]} = \frac{2m^2B_1B_3 + 3m^3B_2(e^{-2\tau} + 1)}{B_1^2B_3(e^{-\tau} - 1)} +$ $+ \frac{B_1B_3m^2 + 3m^3B_2(me^{-\tau} + 1)}{B_1^2B_3} + \frac{B_2m^3}{B_1B_3}$

Table 2-1. continued

$$x_{o,3} = x_o^{[3]} = \frac{-3m^3(e^{-2\tau} + 1)}{B_1 B_3(e^{-\tau} - 1)} - \frac{3m^3(me^{-\tau} + 1)}{B_1 B_3} - \frac{m^3}{B_3}$$

$$J_3 = \frac{1}{\tau}\left\{(1-e^{-\tau})x_{o,1} + (e^{-\tau} - \frac{e^{-2\tau}}{2} - \frac{1}{2})x_{o,2} + (-e^{-\tau} + e^{-2\tau} - \frac{e^{-3\tau}}{3} + \frac{1}{3})x_{o,3}\right\}$$

where

$$B_1 = e^{-\tau}(e^{-\tau} - 2m) - 1$$

$$B_2 = [2e^{-\tau}(e^{-\tau} - 1)](e^{-\tau} - m)$$

$$B_3 = e^{-3\tau} + 3m^2e^{-\tau}(e^{-\tau} - 1) - 1 - \frac{6m(me^{-\tau} + 1)(e^{-\tau} - m)(e^{-\tau} - 1)e^{-\tau}}{e^{-\tau}(e^{-\tau} - 2m) - 1}$$

$$B_4 = e^{-\tau}(e^{-\tau} - \frac{B_2}{B_1} - 1)$$

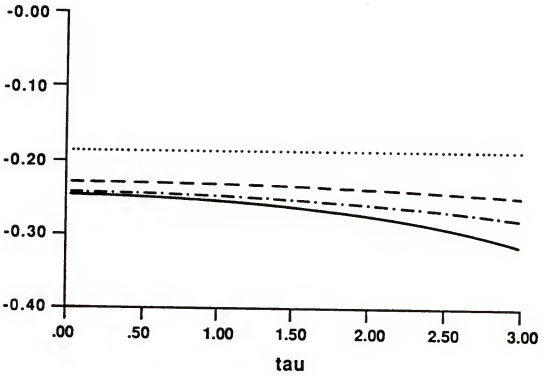

Figure (2-3). Effect of the period τ on the performance measure J. The exact solution (——) is compared to the first (...), second (---) and third (.-.-) order approximation.

Conclusions

The new method proposed allows to solve for optimal impulsed forcing analytically by employing the Carleman linearization procedure. The quality of the approximation is excellent, depending on the order of the Carleman linearization procedure used. This method is limited to systems or regions of systems, where inflicting disturbances with a period τ lead to τ-periodic output.

CHAPTER III
APPLICATIONS IN BIOCHEMICAL ENGINEERING

III. 1. Periodic Optimization of Continuous Microbial Growth Processes

Introduction

Very little work in biochemical engineering has been done with continuous reaction systems. And not surprisingly even less work has been done in control and optimization of biochemical reactors. However, over the past few years continuous fermentations have dramatically increased in significance and hence their optimization becomes very important.

As mentioned in Chapter I, periodic reactor operation is often superior to steady-state operation, which gives great significance to the problem of periodic optimization of continuous microbial growth processes.

The objective of this work is to apply the π-criterion to microbial growth systems in a continuous chemostat culture. In particular two different problems are addressed. The first consists of optimization of the total biomass productivity, based on dynamic models of the chemostat. The second problem to be addressed is the maximization of the productivity of protein based on a structured model due to Williams.

Periodic Optimization of Biomass Production

The proper choice of the performance measure is perhaps the most important decision in any optimization process. For processes that have as an objective the production of biomass, the total biomass productivity (in grams per unit time per unit volume) as represented by the product Dx, where D is the dilution rate and x the biomass concentration, should be included in the performance measure. Since the limiting substrate constitutes the major running cost, a reasonable performance measure is

$$J = Dx - qDS^{o} \tag{3-1}$$

where S^{o} is the feed substrate concentration, and q is the relative cost of the substrate. All mathematical models of the chemostat that have appeared in the literature, whether unstructured [38-40] or structured [41-48], predict that J is maximum at a unique value of the dilution rate D. This optimum dilution rate lies between 0 and the maximum specific growth rate μ_m at the prevailing culture conditions. The existence of an optimal dilution rate has also been verified experimentally [49-52].

The question arises whether periodic variation of the dilution rate can lead to enhanced performance when compared with the optimum steady-state operation. This possibility is investigated in the current work employing both structured and unstructured models.

The simplest possible model type, an unstructured model, has inherent the assumption of "balanced growth" [53]. Following this assumption, the dynamics of the chemostat can be described by the following general two-dimensional system of equations:

$$\frac{dx}{dt} = \mu(s,x)x - Dx \tag{3-2}$$

$$\frac{ds}{dt} = -\frac{\mu(s,x)x}{Y} + D(S^o - s) \tag{3-3}$$

where x and s are the concentrations of biomass and substrate respectively, μ is the specific growth rate and Y is a yield factor. Most of such unstructured models (with the exception of a model due to Contois [54]) assume that μ is a function of s only. By far the most commonly used model is that due to Monod [38]. It assumes the following functionality for the specific growth rate:

$$\mu(s) = \frac{\mu_m s}{K_s + s} \tag{3-4}$$

where μ_m is the maximum growth rate at the culture temperature and pH, and K_s is a constant. For the Monod model (equations (3-2) to (3-4)) the optimal dilution rate for steady-state operation is given by

$$D_{opt} = \mu_m \left(1 - \sqrt{\frac{K_s}{K_s + S^o(1 - \frac{a}{Y})}}\right) \tag{3-5}$$

Consider now the periodic optimization problem. It is assumed that D is varied periodically with an average equal to D_{opt}. The π-criterion can be used to test the desirability of such operation. In this case equation (2-1) takes the form of equations (3-2) and (3-3) with $\mu(s)$ given by (3-4), u=D (the control variable), $x_1=x$, $x_2=s$ (the state variables) and y=x (i.e. it is assumed that the biomass concentration is the measured variable). The performance measure is given by equation (3-1), and an equality constraint of the form (2-21) is relevant with

$$v = DS^o - c \tag{3-6}$$

where c is a constant. This requires that the total average feed is fixed. The Hamiltonian function in this case is

$$H = Dx - qDS^o + \lambda_1\left(\frac{\mu_m sx}{K_s + s} - Dx\right) + \lambda_2\left(-\frac{\mu_m sx}{Y(K_s + s)} + D(S^o - s)\right) + \mu(DS^o - c) \tag{3-7}$$

Using equations (3-2) - (3-7) with q=0, $\pi(\omega)$ is found to be

$$\pi(\omega) = -2x^2 \frac{\frac{\mu_m K_s \omega^2}{Y(K_s + s)^2} + \frac{D\omega^2}{Y(K_s + s)} + \frac{D^2 \mu_m K_s}{Y(K_s + s)^2} + \frac{D^3}{Y(K_s + s)}}{\left(\frac{DK_s \mu_m x}{Y(K + s)^2} - \omega^2\right)^2 + \left(\frac{K_s \mu_m x\, \omega}{Y(K + s)^2} + D\omega\right)^2} \tag{3-8}$$

where all variables are evaluated at their steady-state values for $D=D_{opt}$. As can be easily seen from equation (3-8), $\pi(\omega)$ is negative for all values of the cycling frequency ω. This means that for a Monod-type model steady-state operation is always superior to cycling, regardless of the cycling frequency.

All unstructured models predict a response to step-changes in operating variables, such as S^0 and D, which is faster than experimentally observed [55]. This is a result of the inherent assumption of those models that there is no time-lag between changes in the substrate level and adjustment of the growth rate at the appropriate level. To relax this assumption one may assume that the specific growth rate is a function not only of the present substrate level but also of previous levels in a weighted manner. In this case the growth rate is taken to be a function of z instead of s, where

$$z = \int_{-\infty}^{t} s(\tau)F(t-\tau)d\tau \qquad (3-9)$$

$F(t-\tau)$ is a memory function that weighs appropriately previous substrate levels. If one chooses

$$F(Y) = \alpha e^{-\alpha Y} \qquad (3-10)$$

then it can be shown [34] that the dynamic equations for the chemostat take the form

$$\frac{dx}{dt} = \mu(z)x - Dx \qquad (3-11)$$

$$\frac{ds}{dt} = -\frac{\mu(s)x}{Y} + D(S^o - s) \tag{3-12}$$

$$\frac{dz}{dt} = \alpha(s - z) \tag{3-13}$$

A similar delay-model was introduced by Wang and Stephanopoulos [56]. The smaller the magnitude of the parameter α, the slower is the response of the growth rate to a change in the level of the substrate. Defining dimensionless variables

$$\hat{s} = \frac{s}{S^o} \; ; \; \hat{x} = \frac{x}{YS^o} \; , \; \hat{K}_s = \frac{K_s}{S^o} \; ; \; \hat{D} = \frac{D}{\mu_m}$$

$$\hat{t} = t\mu_m \; ; \; \hat{z} = \frac{z}{S^o} \; ; \; \hat{\alpha} = \frac{\alpha}{\mu_m}$$

the dynamic equations take the form

$$\frac{d\hat{x}}{d\hat{t}} = \frac{\hat{z}\hat{x}}{\hat{K}_s + \hat{z}} - \hat{D}\hat{x} \tag{3-14}$$

$$\frac{d\hat{s}}{d\hat{t}} = -\frac{\hat{s}\hat{x}}{\hat{K}_s + \hat{s}} + \hat{D}(1 - \hat{s}) \tag{3-15}$$

$$\frac{d\hat{z}}{d\hat{t}} = \hat{\alpha}(\hat{s} - \hat{z}) \tag{3-16}$$

The performance measure takes the form

$$\hat{J} = \hat{D}\hat{x} - \hat{D}(1 - \beta) \tag{3-17}$$

where $\beta = 1 - \frac{q}{Y}$

The optimal dimensionless dilution rate is

$$\hat{D}_{opt} = 1 - \frac{\hat{K}_s}{\hat{K}_s + \beta} \tag{3-18}$$

The Hamiltonian in this case becomes

$$H = \hat{D}\hat{x} - \hat{D}(1 - \beta) + \lambda_1\left(\frac{\hat{z}\hat{x}}{\hat{K}_s + \hat{z}} - \hat{D}\hat{x}\right) + \lambda_2\left(-\frac{\hat{s}\hat{x}}{\hat{K}_s + \hat{s}} + \hat{D}(1 - \hat{s})\right)$$

$$+ \lambda_3\hat{\alpha}(\hat{s} - \hat{z}) + \mu(\hat{D} - \hat{c}) \tag{3-19}$$

The expression for $\pi(\omega)$, which is again a scalar function, is given in Appendix D. It is a function of only three variables $\hat{K}_s$, $\hat{\alpha}$ and β.

To test the effect of the delay $\hat{\alpha}$ and the cost factor β, π was evaluated numerically and plotted as a function of ω. When q=0 (implying β=1), the effect of delay alone may be seen in Figure 3-1. It is seen that $\pi(\omega)$ becomes positive for a range of cycling frequencies ω, resulting in enhanced performance. It was also found that the greater the time delay (i.e. the smaller $\hat{\alpha}$), the higher is the maximum of $\pi(\omega)$ and the lower the value of ω at which it occurs. Large values of $\hat{\alpha}$ result in an all-negative $\pi(\omega)$ in agreement with the Monod model without delay (equation 3-8). Figure 3-2 shows the effect of the dimensionless cost factor β. As β increases, the maximum of $\pi(\omega)$ decreases and occurs at higher cycling frequencies. Therefore, higher nutrient

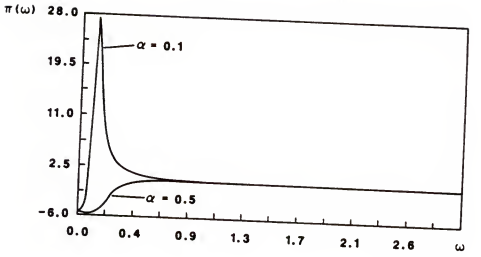

Figure (3-1). $\pi(\omega)$ versus ω for Monod-model with delay as given by equation (3-10) and cost factor (dimensionless) Model parameters: K_s =0.9, β= 1., α= 0.1,0.5

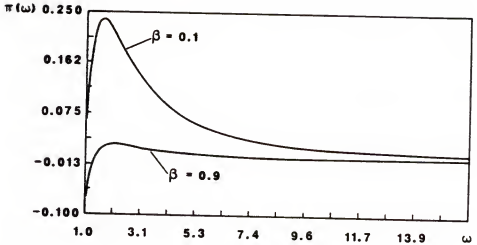

Figure (3-2). $\pi(\omega)$ versus ω for Monod-model with delay as given by equation (3-10) and cost factor (dimensionless). Model parameters: K_s=0.9, α=1., β=0.1, 0.9.

costs improve the effectiveness of cyclic operation. Notice also from equation (3-18) that whenever q is greater than Y, the optimum dilution rate is zero, implying that in this case a batch operation is of choice. Finally, it should be noted that for very large cycling frequencies, $\pi(\omega)$ goes to zero, implying that the cyclic operation results in an average performance measure equal to that of the optimum steady-state operation. This is expected because for very fast cycling, the culture does not have the time to respond to periodic variations, so it reacts to the average D, which is D_{opt}, and the performance measure J approaches the optimal steady-state value J^{O} as $\omega \to \infty$.

If in place of equation (3-10) the memory function

$$F(Y) = \delta(Y - \tau) \tag{3-20}$$

is chosen (δ being the Dirac delta function), a somewhat different behavior is observed. In this case growth depends on the substrate level at a particular instant in the past. The state equations are equation (3-11) and (3-12) with

$$z = s(t - \tau) \tag{3-21}$$

This model is a two-dimensional system of delay-differential equations. For such systems, a π-criterion was derived by Sincik and Bailey [23]. Their results were used to find an expression for $\pi(\omega)$ which is given in Appendix E. For this delay model, more than one frequency range is found for which $\pi(\omega) > 0$. The situation is exemplified in Figure 3-3. This behavior is in agreement with some experimental findings [15].

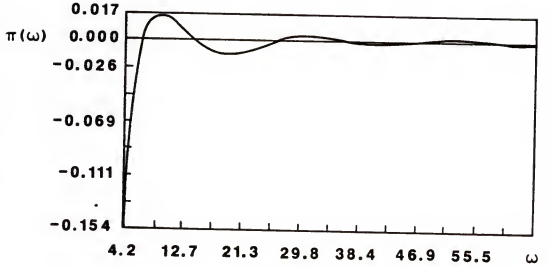

Figure (3-3). $\pi(\omega)$ versus ω for Monod model with delay as given by equation (3-20). Model parameters: μ_m=0.7, Y=0.5, K_s=22., S^o=30., τ= 0.3

To verify the predictions of the π-criterion, numerical simulations were undertaken. Square-wave variations (bang-bang switches) around the optimal dilution rate were employed, rather than sinusoidal variations, since such type of cycling has previously proven superior and easier to implement experimentally. Figure 3-4a is a plot of the ratio of performance measures ($J_{cycling}/J_{steady\text{-}state}$) versus cycling frequency for the system described by equations (3-14)-(3-16) (with $\hat{\alpha} = 0.1$, $\hat{\beta} = 0.65$ and $\hat{K}_s = 0.5$). The amplitude of the square-wave was chosen to be 0.5 D_{opt}. For comparison purposes a plot of $\pi(\omega)$ is also shown (Figure 3-4b). The simulations predict remarkable improvement in process performance. Moreover, the optimal cycling frequency as obtained by intergration is seen to be close to that predicted by the π-criterion.

Periodic Optimization of Protein Production

In the previous section time-delay models were used to describe the dynamics of the chemostat. An alternative type of structured modeling which realizes that under dynamic conditions balanced growth is not valid could be used instead. Such structured modeling has been found, in general, superior in describing the dynamics of the chemostat. The simplest structured model is that due to Williams [41].

The fundamental assumption of the Williams model is that the cell consists of two basic components, one synthetic and one structural/genetic. The synthetic portion includes the sum total of small metabolites in the cell and the ribosomes (RNA), whereas the greater bulk of the structural/genetic portion is protein and DNA. Although the exact physical significance of the variables in the Williams-model has not been established, the predictions of this model are still worth considering. Williams's model in dimensionless form may be written as

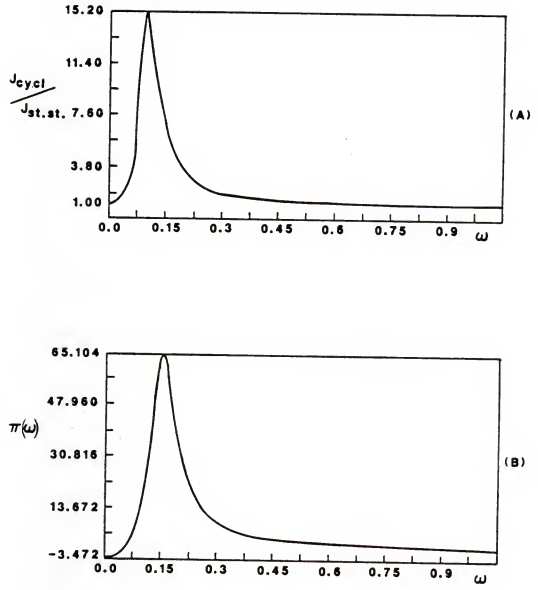

Figure (3-4). Predictions for the optimal cycling period
a) $J(\omega)$ versus ω for Monod-model with delay as given by equation (3-10) and cost factor (dimensionless). Model parameters: K_s =0.5, =0.1, =.65, D_{opt} =0.34.
b) $\pi(\omega)$ versus ω. Model parameters as in a).

$$\frac{d\tilde{x}_1}{d\tilde{t}} = \tilde{x}_1\tilde{x}_2 - \tilde{D}\tilde{x}_1 \tag{3-22}$$

$$\frac{d\tilde{x}_2}{d\tilde{t}} = -\tilde{x}_1\tilde{x}_2 + (1 - \tilde{x}_2)\tilde{D} \tag{3-23}$$

$$\frac{d\tilde{x}_3}{d\tilde{t}} = \frac{\tilde{x}_3(\tilde{x}_1 - \tilde{x}_3)}{\tilde{\alpha}} - \tilde{D}\tilde{x}_3 \tag{3-24}$$

where $\tilde{x}_1$ is the dimensionless biomass concentration, $\tilde{x}_2$ is dimensionless substrate concentration and $\tilde{x}_3$ is the dimensionless concentration of the structural/genetic portion. In particular

$$\tilde{x}_1 = \frac{x_1}{S^o} \; ; \; \tilde{x}_2 = \frac{x_2}{S^o} \; , \; \tilde{x}_3 = \frac{x_3}{S^o} \; ; \; \tilde{t} = tK_1S^o$$

$$\tilde{D} = \frac{D}{K_1S^o} ; \; \tilde{\alpha} = \frac{K_1}{K_2}$$

where K_1 and K_2 are kinetic constants of the original Williams model.

The structural/genetic portion consists mainly of protein, the DNA content being relatively small. Thus we can loosely assume that $\tilde{x}_3$ is the dimensionless concentration of protein in the culture.

We are interested in operating the chemostat in a manner which is optimum for the production of protein. That is in this case the performance measure is

$$\tilde{J} = \tilde{D}\tilde{x}_3 \tag{3-25}$$

The optimum dilution rate for steady-state operation in this case is calculated to be

$$\tilde{D}_{opt} = \frac{1}{2(1 + \tilde{\alpha})} \tag{3-26}$$

The optimization is again subject to the equality constraint (3-6). Taking u=D, $\underline{x} = (\tilde{x}_1, \tilde{x}_2, \tilde{x}_3)^T$ and y=$\tilde{x}_3$, the Hamiltonian in this case becomes

$$H = \tilde{D}\tilde{x}_3 + \lambda_1(\tilde{x}_1\tilde{x}_2 - \tilde{D}\tilde{x}_1) + \lambda_2(-\tilde{x}_1\tilde{x}_2 + (1-\tilde{x}_2)\tilde{D}) + \lambda_3\left(\frac{\tilde{x}_3(\tilde{x}_1 - \tilde{x}_3)}{\tilde{\alpha}} - \tilde{D}\tilde{x}_3\right) + \mu(\tilde{D} - c) \tag{3-27}$$

$\pi(\omega)$ is again a scalar and the appropriate expression is given in Appendix F. A graphic illustration is given in Figure 3-5. From this figure it can be seen that cycling results in improved performance. It should be noted that as $\tilde{\alpha}$ increases, the optimum forcing frequency decreases. Numerical simulations have verified the global validity of these results.

Conclusions

The π-criterion is a very useful method for determining whether periodic operation can lead to superior bioreactor performance. Enhanced productivity of biomass results when a bioreactor is operated

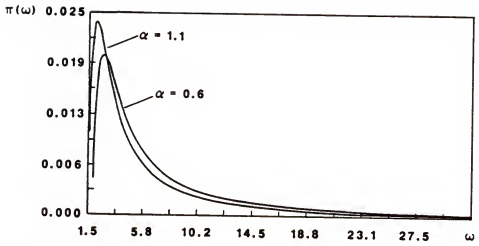

Figure (3-5). $\pi(\omega)$ versus ω for Williams' model. Model parameters: $\tilde{\alpha}$=0.6, 1.1

with a periodically varying dilution rate. This is a consequence of the fact that there is a time lag in the culture adaptation to a new growth level whenever a disturbance is introduced. Finally structured models such as the Williams' model that relax the assumption of "balanced growth," predict an increase in the average protein productivity upon periodic variation of the dilution rate.

Chapter III. 2. The Effect of Periodic Forcing on Saccharomyces cerevisiae in Continuous Culture

Introduction

As mentioned in Chapter 1, continuous operation of bioreactors has only become important over the past few years. Thus, although a substantial amount of work has been undertaken for the optimization of batch processes [1-6] only very little has been done for the optimization of continuous bioreactors [7], even less so in the area of periodic reactor operation.

A few workers have conducted experiments to observe the behavior of chemostat cultures when subjected to cyclic operation. The major references are summarized in Table 3-1 [15-20, 57, 58]. It is hard to draw general conclusions from those first attempts to assess the effect of cycling experimentally. In many cases, complex (e.g. undefined) growth media like molasses were used or some quantities, such as yield factors have either been not well defined or defined differently. In these experiments the limiting substrate concentration or the dilution rate served as the manipulated process variable.

Picket, Bazin and Topiwala [15] (using S^o, the feed limiting substrate concentration as control variable) found that at some frequencies periodic reactor operation was superior to steady-state operation.

Table 3-1. Summary of Major References on Experiments Involving Periodic Reactor Operation

Reference No.	Culture Type	Control Variable	Wave form	Variation of	Effect on Average Biomass Yield
17	E. Coli/glucose	S_o	Squarewave	Frequency	higher than s.s. in some frequency ranges
15	E. Coli/glucose	S_o	Squarewave	Amplitude	increasing function of amplitude
16	S. Cerevisiae/ molasses	S_o	Squarewave + Sinusoidal	Amplitude & Frequency	small effect if any
57	E. Coli/glucose	S_o	Sinusoidal	Frequency	not reported
18	S. Cerevisiae/ molasses	D	Varying	Form of Oscillation	none
19	K. Aerogenes/ glucose	D	Sinusoidal	Frequency	not reported
55	S. Cerevisiae/ glucose	D	Sinusoidal	Amplitude	not reported

Moreover, the observed improvement in these frequency-ranges was found to increase with increasing cycling amplitudes.

It has been known for some time that the concentration of some important metabolites inside the cell is not constant during a dynamic process. It has also been observed that the average macromolecular composition of the cell changes under cyclic conditions [17]. So it was found that the percent composition of protein and RNA (essential for growth) is higher when periodic operation is employed. Especially in the case where protein is an economically important factor this result is of considerable significance.

The purpose of this study is to observe the behavior of S. cerevisiae in continuous culture undergoing square wave forcing in the dilution rate. After a steady-state model has been obtained from steady-state data, a dynamic model is found which succeeds in describing the response of the system to step changes in the dilution rate. Subsequently experiments are performed to observe the behavior of the culture under periodic conditions.

In the next section the experimental apparatus, materials and methods will be described. Thereafter the steady-state as well as the dynamic response experiments are described and it is shown how a mathematical model was derived from the obtained data. The last part of Chapter 3 is concerned with the periodic optimization of the bioreactor, in theory and in experiment.

Equipment

A schematic representation of the experimental system is given in Figure 3-6.

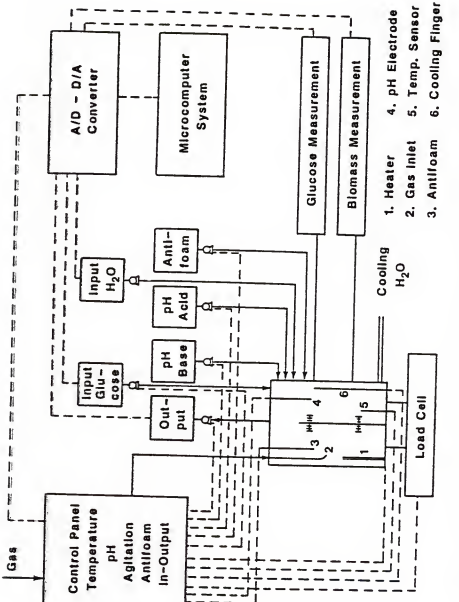

Figure (3-6). A schematic representation of the experimental system

The Bioengineering KLF 2000 fermentor with 3 liter glass cylinder serves as chemostat. The average reactor volume is 2.5 lt. A DC motor driven from below rotates axially two flat blade agitators. Mixing is enhanced by steam breakers inside the vessel. The agitation system is connected with the control panel for speed measurement and setting. The rotation speed was kept at 500 rpm. The top of the vessel has access ports for pH measurement and control, DO-electrode, foam sensor and control, aeration, addition of the growth medium and an additional port for re-entry of a recycle loop for the turbidity measurement. The bottom plate of the fermentor has two ports, one for harvesting and one for the recycle loop.

The temperature is controlled via a temperature controller located in the control panel. A pt 100 temperature sensor monitors the fermentation temperature continuously. An 800 W heating finger keeps the temperature at 30°C, the optimal growth temperature for yeast.

The pH controller also located at the control panel is quasi steady-state three-point eliminator. A silver/silver chloride electrode is inserted through the top of the vessel and monitors the pH continuously. The controller keeps the pH inside the fermentor at 4.0 through actuating two peristaltic pumps that deliver either NaOH or HCl as needed.

The available pumps are constant flow rate pumps. In continuous steady-state operation of the harvesting pump is set for a certain flowrate and not controlled, the feed pump is controlled by the load-cell control system (on/off).

A turbidity measurement device is employed for the continuous measurement of the optical density, from which the concentration of

biomass can be obtained. The TMK turbidity monitor by bioengineering is equipped with a flow-through cuvette through which the recycle stream is guided.

A continuous glucose analyzer from Analytical Research was used for continuous glucose measurement. Periodically a small amount of the medium is sampled and led to the analyzer. At the end of an electrochemical sensor rests an immobilized enzyme membrane. The enzyme catalyzes the reaction between the sugar and oxygen to form H_2O_2 which is detected by the sensor.

A PDP 11/23 microcomputer equipped with a 10 M hard disk drive, a graphics terminal and an LA 100 printer together with Data Translation AD/DA converters comprises a complete data acquisition, manipulation and agitation system, to be used on-line for direct digital control. For the case of periodic squarewave forcing the computer has been programmed to control the harvest pump in an on/off manner. The control panel adjusts the feed pump to keep the reactor volume constant.

Materials and Methods

S. cerevisiae was obtained from the Department of Microbiology at the University of Florida. Stock cultures were maintained on nutrient broth agar at 8°C. The composition of the feed medium for continuous operation is listed in Table 3-2. To avoid the possibility of a change in the feed composition through a chemical reaction, batches I and II were autoclaved separately and mixed under UV-light. For the start-up proceedings batch II was sterilized in the fermenter at 121°C for 30 minutes, batch I was autoclaved and used as a seed flask for the reactor.

Table 3.2. Composition of the Growth Medium

	Substance	Concentration
I	Glucose	2 g/ℓ
	Yeast Extract	.2 g/ℓ
	$MgSO_4 \cdot 7H_2O$	.4 g/ℓ
II	Potassium Phosphate monobasic	5 g/ℓ
	Ammonium Sulfate	2 g/ℓ

Dry weights of cell mass were obtained by heat-shocking 50 ml of sample for 6 minutes to inhibit further growth, followed by centrifugation (30 minutes at 1200 rpm). The liquid was decanted and the cells washed with distilled water. After suspending them in 2 ml of distilled water they were poured in open petri-dishes and the water was gently evaporated.

Establishment of a Steady-State Model

The material balances for the chemostat can be described by the following two-dimensional system of equations (unstructured model)

$$\frac{dx}{dt} = \mu(s)x - Dx \tag{3-28}$$

$$\frac{ds}{dt} = -\frac{1}{Y}\mu(s)x + D(S^o - s) \tag{3-29}$$

where x and s are the concentrations of biomass and substrate, respectively, μ is the specific growth rate and Y the yield factor

$$Y = \frac{\text{grams biomass produced}}{\text{grams glucose used}} \tag{3-30}$$

The unstructured model due to Monod [38] assumes the following functionality for the specific growth rate

$$\mu(s) = \frac{\mu_m s}{K_s + s} \tag{3-4}$$

μ_m being the maximum growth rate at the given culture conditions and K_s being a constant. The model used to describe the steady-state behavior of the system therefore is

$$\frac{dx}{dt} = \frac{\mu_m s}{K_s + s} x - Dx \tag{3-31}$$

$$\frac{ds}{dt} = -\frac{1}{Y} \frac{\mu_m s}{K_s + s} x + D(S^o - s) \tag{3-32}$$

At steady state equation (3-31) can be rewritten as

$$\frac{1}{D} = \frac{K_s}{\mu_m} \cdot \frac{1}{s} + \frac{1}{\mu_m} \tag{3-33}$$

This functionality can be used to determine the constants μ_m and K_s by plotting 1/D versus 1/s (also known as Lineweaver-Burk plot). Table 3-3 summarizes the steady-state measurements of the system.

Table 3-3. Summary of the Steady-State Behavior

Dilution Rate [hr^{-1}]	Biomass Concentration [g/L]	Substrate Concentration [g/L]
0.100	.275	.460
0.104	.290	.403
0.116	.268	.530
0.154	.173	.802
0.200	---	1.196
0.209	.133	1.181

Figure 3-7 shows the Lineweaver-Burk plot obtained from steady-state data. Given the culture conditions described in the previous sections and using linear regression the constants were found to be

$$\mu_m = 0.5574$$
$$K_s = 2.0535$$
$$Y = 0.175$$

The Response of the System to a Step Change in the Dilution Rate

The Monod-model, although it succeeds in describing the chemostat at steady-state in most cases, is known to fail to predict dynamic responses accurately. Figure 3-8 proves this to be true for the system at hand. The response of the biomass in grams/liter is followed over time after a step change in the dilution rate from 0.2 to 0.1 has been performed. As can be seen clearly, the Monod-model is not only too

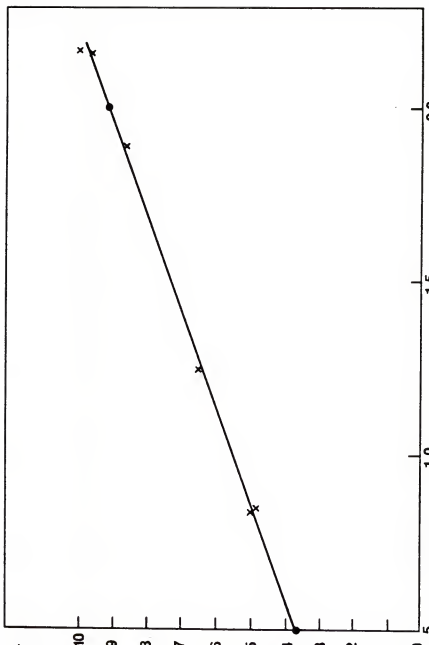

Figure (3-7). Lineweaver - Burk plot for the determination of the constants K_s and μ_m in the Monod-model

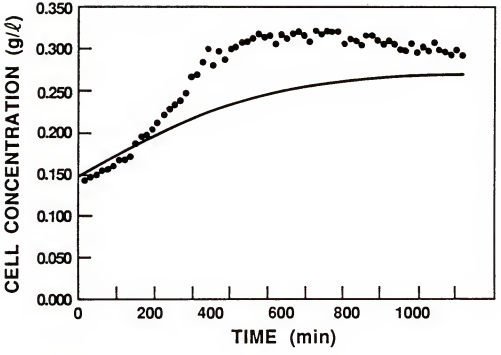

Figure (3-8). The response of the biomass to a step-change in the dilution rate from 0.2 to o.1; the predictions of the Monod-model

sluggish to portray the fast initial response of the culture, it also fails to predict the overshoot and subsequent return to the steady-state value corresponding to the new dilution rate. This is due to the inherent assumption of this model, that there does not exist a time-lag between a change in the substrate concentration and adaptation of the culture for growth at the new substrate level.

To relax this assumption, a time-delay was introduced in the model (see Chapter III.1.). Equation (3-9) was used and the best fit to the experimental data was found for the case of a pure time-delay, i.e. choosing equation (3-20) as memory function. An equivalent way to formulate the pure time-delay in a form which is convenient for numerical simulations is (for high enough k [59])

$$\frac{dx}{dt} = \frac{\mu_m z_1 x}{k_s + z_1} - Dx \tag{3-34}$$

$$\frac{ds}{dt} = -\frac{1}{y}\frac{\mu_m s x}{k_s + s} + D(S^o - s) \tag{3-35}$$

$$\begin{aligned}
\frac{dz_1}{dt} &= \alpha(z_2 - z_1) \\
\frac{dz_2}{dt} &= \alpha(z_3 - z_2) \\
&\vdots \\
\frac{dz_k}{dt} &= \alpha(s - z_k)
\end{aligned} \tag{3-36}$$

α being an adaptability parameter. It was found that k = 10 is sufficiently large. Given the Monod-parameters obtained in the previous section, it was attempted to find the value of the adaptability

parameter α which would give the best fit to the experimental data, as judged by the "least-square-error." If one tries to obtain the best fit to all the data until the transients have virtually subsided (1,020 minutes), the optimal α is found to be 3. As seen in Figure 3-9 the fit is not in very good quantitative agreement with the experimental step response, especially in describing the initial steep increase, but such a delay model is able to predict a faster rise in biomass than the Monod-model. This is a result of the specific growth rate continuing to be high for a certain period of time, following a step down in the dilution rate. On the other hand, if the objective is to describe the initial steep response as accurately as possible, a much lower value for α, i.e. 1, should be chosen. But, as Figure 3-10 indicates, using this high value for the time-delay predicts an overshoot in the biomass concentration, which is unacceptable.

From the physiological point of view, it is well established that a culture enters a so-called "lag-phase" when it is subjected to different environmental conditions. It utilizes this time to adapt its metabolism to the new environment. After this adaptation has taken place it responds much more actively to the environment. Incorporating this effect in the model allows to describe the step response successfully. Using the model as described by equations (3-34) to (3-36) and

$$\begin{aligned} \alpha &= 1. \quad \text{for} \quad t < 3 \text{ hours} \\ \alpha &= 4. \quad \text{for} \quad t \geq 3 \text{ hours} \end{aligned} \tag{3-37}$$

gives the result as seen in Figure 3-11.

Now consider a step change in the dilution rate in the opposite direction, from 0.1 to 0.2. Figure 3-12 shows once more that the Monod

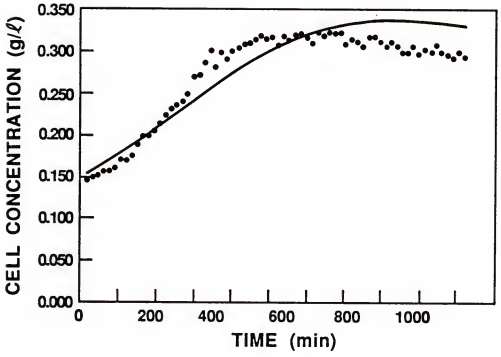

Figure (3-9). The response of the biomass to a step-change in the dilution rate from 0.2 to 0.1; the predictions of a pure time-delay model (α=3.)

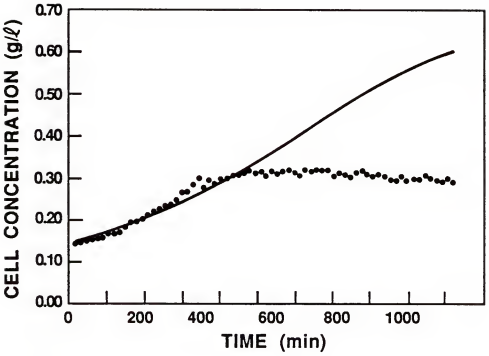

Figure (3-10). The response of the biomass to a step-change in the dilution rate from 0.2 to 0.1; the predictions of a pure time-delay model (α=1.)

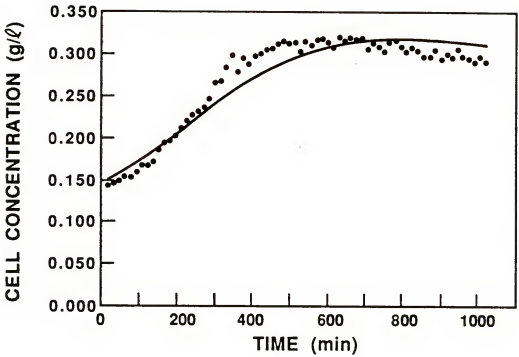

Figure (3-11). The response of the biomass to a step-change in the dilution rate from 0.2 to 0.1 ; the predictions of the model which incorporates a change in the physiological state of the culture

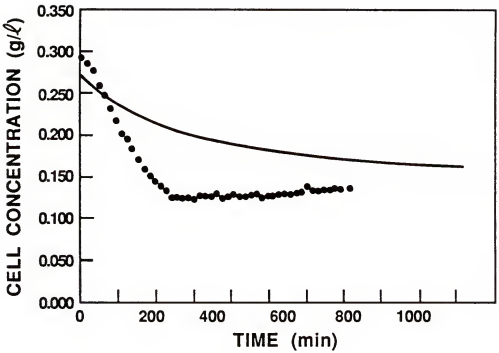

Figure (3-12). The response of the biomass to a step-change in the dilution rate from 0.1 to 0.2; the predictions of the Monod-model

model describes a response which is much too slow. But in this case (Figure 3-13) even the pure time-delay model, which incorporates a shift in the physiological state of the culture, although predicting a faster response, does not succeed in accurately portraying this step response. After analyzing the data it was concluded, that, after the dilution rate was stepped up from 0.1 to 0.2, all growth has stalled. As Figure 3-14 proves, the drop in the biomass-concentration corresponds exactly to the one expected for zero growth rate, leaving only the hydraulic effect of the culture being washed out of the fermenter.

It might seem surprising at first that growth should be arrested following a step up in the dilution rate, but this state of shock can be compared to the one where an inoculum is placed into new medium. Again, the culture reacts by entering a lag-phase to adapt to the new environment. As the previous figures indicate, growth starts to reoccur after a certain time. And, not surprisingly, this time is about three hours, thus agreeing with the length of the lag-phase for a step change down in dilution rate. The length of the lag phase very likely is a function of the magnitude of the step change, being virtually zero for small steps and higher for larger ones.

The Response of the System to Periodic Variation of the Dilution Rate

Starting from a steady-state corresponding to a dilution rate of 0.1, the system was subjected to square wave variations in the dilution rate of different periods. The amplitude was twice this dilution rate; i.e. variations from $D = 0.2$ to $D = 0.0$ (batch operation) were implemented, so that the total amount of substrate over a period equals the one at steady-state operation with $D = 0.1$.

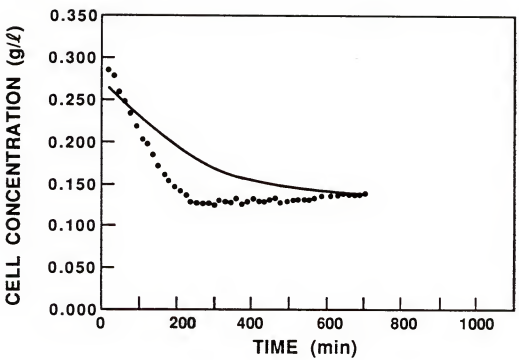

Figure (3-13). The response of the biomass to a step-change in the dilutionrate from 0.1 to 0.2; the predictions of the model, which incorporates a change in the physiological state of the culture

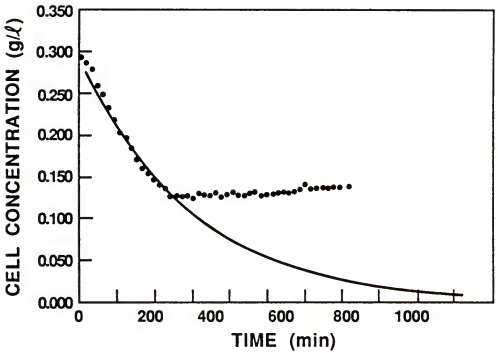

Figure (3-14). The response of the biomass to a step-change in the dilution rate from 0.1 to 0.2; the response as it would be observed for zero growth rate (washout)

From the step-response experiments, which indicated a time-lag of about three hours, it was concluded that a cycling period in the vicinity of three hours might influence the performance of the syste positively. Applying the model established in the previous section, qualitative agreement is found. Cycling with a period of two hours is expected to yield lower productivities than steady-state operation, cycling with a period of three hours higher ones. This modeling is not applicable to the four-hour period because the model does not account for a possible entry into the stationary phase for high periods.

Figure 3-15 presents the results (after all transients have subsided). While cycling with a period of either two or four hours does not produce as much biomass as steady-state operation, cycling with a period of three hours results in significantly improved reactor performance. Table 3-4 lists the concentrations during the cycle and the productivities.

Table 3-4. Biomass Concentrations and Productivities During Cyclic Reactor Operation

τ	Concentration [g/ℓ] low	high	Productivity [g/hr]
2	0.15	0.22	0.0518
3	0.29	0.40	0.0952
4	0.09	0.13	0.0305
steady state (D = 0.1)	0.275		0.0756

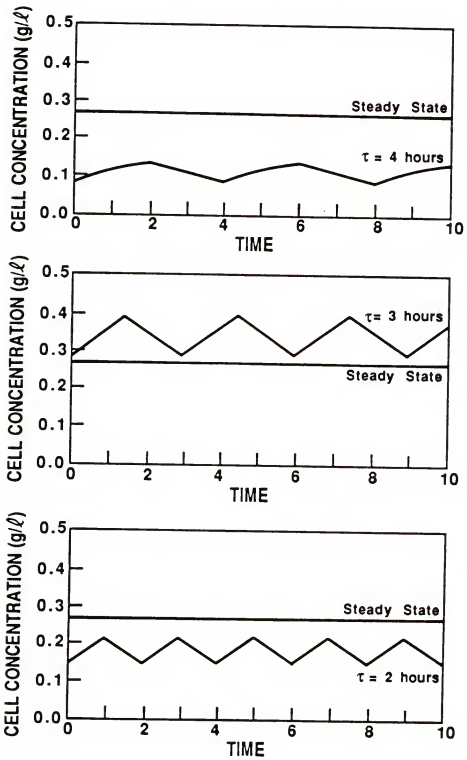

Figure (3-15). Biomass concentration versus time for different cycling periods

The improvement observed at a cycling period of three hours is quite remarkable. During the half of the cycle when the dilution rate is equal to zero, essentially batch growth, the culture clearly is in a state of exponential growth and during the remainder, when the dilution rate is high, growth has stalled. This confirms the observations made in the step change experiments. The magnitude of the improvement might be explained by the fact that, in this case, a high (exponential) growth rate coincides with a high concentration of biomass at a time where there is ample substrate present.

At a cycling period of four hours, as Figure 3-15 shows, the culture is not in a state of exponential growth during the half of the cycle when batch operation prevails. The leveling-off of the slope indicates entry into the stationary phase, while once again, no growth is found for the rest of the cycle. The culture thus switches between nearly stationary phase and lag-phase, not optimal conditions to operate under. That explains the very low productivity at this cycling frequency.

The reduced productivity at a period of two hours might be caused by the fact that the culture is subjected to a change in the environmental conditions too frequently and does not have time to recover during the repeated shocks.

Conclusions

Subjecting the culture to a sudden step up in dilution rate causes it to enter a lag-phase during which growth is temporarily halted. A step down in dilution rate has a similar effect; a lag-phase of about equal length is found during which the growth rate remains close to that

before the change. Thereafter the culture adapts to the new environment.

The same responses are observed when the system undergoes square wave variations in the dilution rate. The reactor performance was found to be inferior to steady-state operation when a cycling period of two or four hours was used, but at a cycling period of three hours a remarkable increase in the biomass productivity was obtained.

CHAPTER IV
APPLICATIONS IN CANCER CHEMOTHERAPY AS AN EXAMPLE FOR DRUG THERAPY

Surgery proves ineffective in over 50% of all cases of cancer where the neoplasms are nonlocalized or diffuse. And so far the success of chemotherapy and radiation therapy has been limited. The limiting factor in cancer chemotherapy (or radiation therapy for that matter) is the toxicity of the antineoplastic agent to the normal, non-carcinogenic cell population. The current approach to determination of a good treatment for an individual in clinical practice is still a trial and error process. Different treatment centers use one and the same drug in as many different ways. Berenbaum [59] proved that a drug successful in reducing the cancer population while keeping the normal cell population above a certain level can easily be classified as ineffective if given the wrong way (even if the overall amount of drug stays the same).

The long overdue methodical search for the optimal treatment regimen can only be done by drawing the complete picture which takes into account both tumor and normal cell kinetics and drug-cell-interaction as well as drug resistance and pharmacokinetics. Given just limited information about the growth history of the tumor and given the pharmacological properties of the drug, a mathematical model will be able to predict the response of tumor and normal cells to chemotherapy and thus allow the choice of the proper drug, dosage and timing.

Mathematical modeling of multicellular organisms, especially as complex ones as the human body, is extremely difficult because many processes at the cellular level like drug-cell interactions and mass transfer limitations, just to name a few, are still not well understood. For the lack of available data and parameters, the model has to be kept as simple as possible. Emphasis is put on clinical application rather than detail. The long term goal is to make use of the kinetic differences between normal and malignant cell populations in order to develop chemotherapeutic protocols with increased selectivity in killing the neoplastic cells. The purpose of this investigation is to establish guidelines for optimal treatment using the limited information available and to show how optimal control theory can be a powerful tool, leading to new approaches in chemotherapy.

IV.1. A Novel Approach for Determining Optimal Treatment Regimen for Cancer Chemotherapy

Introduction

It has frequently been questioned whether continuous or periodic treatment renders the highest effectiveness. The problem of determining the optimum periodic operation for a process described by ordinary differential equations was addressed by Bittanti et al. [22] who developed the so called π-criterion for optimality. As explained in Chapter II.1., this criterion states a sufficient condition for improvement of the performance of a dynamic system via cycling and in addition provides an estimate of the optimum cycling frequencies for the particular system of interest.

The objective now is to investigate the consequences of the π-criterion for cancer chemotherapy. A procedure will be given for determining for a certain patient and a given drug whether continuous or periodic treatment will give better results and for finding the optimal time on/off the drug. The next section sets the mathematical framework for studying the posed optimization problem. The subsequent sections present the results of applying the π-criterion to this physiological system.

Establishment of a Suitable Mathematical Model and Performance Measure

As mentioned earlier, the limiting factor in cancer chemotherapy is the toxicity of the drug to the "limiting tissue," normal homeostatically controlled body cells. Although all body cells are affected by the drug, there is one "limiting tissue" which in most cases is the bone marrow or the intestinal cells. Therefore two cell populations have to be modelled, the neoplastic and the limiting tissue cells.

The following cellular material balances may be written for both cell types:

$$\frac{d\hat{x}_i}{d\hat{t}} = f_i(\hat{x}_i) - g_i(\hat{c})\hat{x}_i \qquad i = c \text{ or } n \tag{4-1}$$

where $\hat{x}_n$ is the normal and $\hat{x}_c$ the cancerous population, $\hat{c}$ is the drug concentration and $\hat{t}$ the time. Several models have been proposed to describe the cellular growth rate functions $f_i(\hat{x}_i)$ [59-65]. For most human tumors the Gompertz equation provides the best fit

$$\frac{d\hat{x}_1}{dt} = A_o - \alpha \ln \frac{\hat{x}_1}{x_o} \qquad A_o, \alpha \text{ ... constants} \qquad (4\text{-}2)$$

It predicts fast exponential growth for a small tumor and slowing growth for increasing tumor size. Several authors [66,67] successfully modelled tumor growth using this equation.

The drug-cell-interaction function $g_i(\hat{c})$ has been modelled either as a linear or a Michaelis-Menten type expression. It is a reasonable assumption that a cell population will exhibit a certain saturation effect towards a drug, so

$$g_i(\hat{c}) = \frac{k_i \hat{c}}{K + \hat{c}} \qquad k_i, K \text{ ... constants} \qquad (4\text{-}3)$$

Swan and Vincent [68] used an equation of this form to model the data on ten patients who had been treated according to the MCP-protocol (Melphalan, Cyclophosphamide, Prednisone). They assumed a single fictitious drug to represent the effect of MCP. The parameters obtained from their data will be employed in this work.

Several authors [61,68,69] solved optimal control problems for cancer chemotherapy. Their result was a desired plasma concentration of the drug versus time at the action site. But these results are of rather limited practical use because they cannot tell a clinician how much medication to administer to a patient or at what time intervals.

An applicable result requires the regimen to be not in terms of plasma drug concentration but in terms of actual dosage. This in turn calls for a relationship which describes the fate of the drug once it

enters the body. The proper pharmacokinetic equation for the case of constant infusion, treating the body as one compartment is [70]

$$\frac{d\hat{c}}{dt} = \hat{u} - \delta\hat{c} \qquad \delta \ldots \text{constant} \tag{4-4}$$

where $\hat{c}$ represents the plasma-concentration and $\hat{u}$ the dosage regimen, which is the manipulated variable for the model adopted in this work. Making the following assumptions:

- Gompertz growth of untreated tumor
- Saturation effect of drug-cell interaction
- First order pharmacokinetics
- One compartment model

The dimensionless model is as follows (Appendix G):

$$\frac{dy_n}{dt} = -\alpha y_n - \frac{\gamma_n c}{1 + c} \qquad \text{normal cell population} \tag{4-5}$$

$$\frac{dy_c}{dt} = -y_c - \frac{\gamma_c c}{1 + c} \qquad \text{tumor cell population} \tag{4-6}$$

$$\frac{dc}{dt} = u - \delta c \qquad \text{drug concentration} \tag{4-7}$$

The steady state this system approaches is given by

$$y_n^o = -\frac{1}{\alpha}\frac{\gamma_n u^o}{\delta + u^o} \tag{4-8}$$

$$y_c^o = -\frac{\gamma_c u^o}{\delta + u^o} \tag{4-9}$$

$$c^o = \frac{u^o}{\delta} \tag{4-10}$$

As can be seen easily from equations (4-8) - (4-10) in connection with Appendix C, if no drug is given ($u^o = 0$) $x_n = x_{n,\infty}$ and $x_c = x_{c,\infty}$, as postulated.

"Steady state" in the strict meaning translates into continuous infusion for this problem. But given the large time constants of this system it can be considered to be at steady state if medication is given daily as opposed to treatment cycles of e.g. 30 days or more. This treatment regimen will be referred to as "continuous treatment."

The proper choice of the performance measure is the most important decision in any optimization process. For this physiological system the objective is twofold:

1. minimize the malignant cell population
2. maximize the benign cell population

In the case of multiple objectives they can be linked to a single performance measure by using 'weighing factors.' However, the choice of these factors requires a value judgement by the scientist, which is

often difficult to make ("How important is it to save normal cells compared to killing tumor cells?"). Therefore it is of utmost importance to choose a performance measure such that the weighting parameter has a physical meaning. It is easy to see that exp $[y_i(t)]$ represents the ratio of the number of cells at time t of treatment divided by the number of cells in the absence of treatment (the maximum attainable number of tumor cells). A proper performance measure is then

$$J = e^{y_n} - qe^{y_c} \tag{4-11}$$

q being a "cost factor." Its physical meaning is the percentage of normal cells the scientist is willing to sacrifice in order to kill 1% of the cancer population. This number might be quite high, for example in cases where bone marrow transplants are possible and very low in other cases.

Optimization of Cancer Chemotherapy

Assume that the behavior of benign cells/malignant cells and the drug can be described by equations (4-5) - (4-7) and the performance measure is given by equation (4-8). The performance measure J is a function of the manipulated variable, the dosage rate u. Figure 4-1 shows the dependence of J on the steady-state value of u. As can be seen clearly there is an optimal steady-state dosage u_{opt}. For the case of continuous treatment the optimal (dimensionless) dosage rate is given by

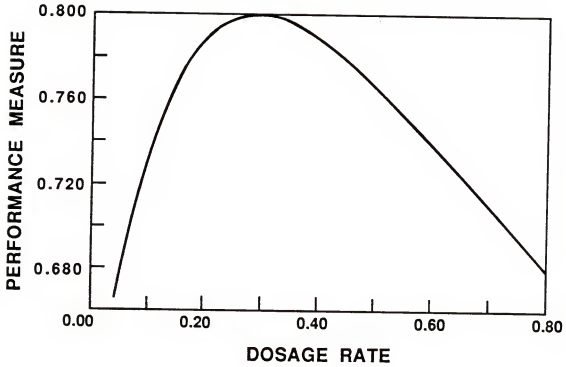

Figure (4-1). Performance measure J versus rate of dosage u. Model parameters: α=10, γ_c=401, γ_n=320.8, δ=66.7, q=0.4

$$u_{opt} = \frac{\alpha\delta\ell n\xi}{\alpha\gamma_c - \gamma_n - \alpha\ell n\xi} \qquad (4\text{-}12)$$

Now consider the periodic optimization problem, i.e. whether enhanced performance is possible upon periodic variation of the dosage. It is assumed that the dosage u is varied periodically with an average equal to u_{opt} as shown in Figure 4-2. The methods of Chapter 2 can be used to test the desirability of such operations. In this case, equation (2-1) takes the form of equations (4-5) - (4-7) with $x_1 = x_n$, $x_2 = y_c$, $x_3 = c$ (the state variables) and $\underline{y} = \underline{x}$ (the outputs being the same as the state variables). The state variables in dimensionless form, for steady state operation (continuous treatment), are given by equations (4-8) to (4-10) by setting $u^o = u_{opt}$. The performance measure, as described in equation (2-19), is given in this case by equation (4-11). Relevant constraints are

$y(\tau) = y(o)$ (outputs are also τ-periodic) (4-13)

$u(t) = u_{max}$ (there is a maximum allowable dosage) (4-14)

$\frac{1}{\tau}\int_o^\tau u(t)dt = u_{opt}$ (total amount of drug over a period is fixed) (4-15)

This gives rise to the Hamiltonian function

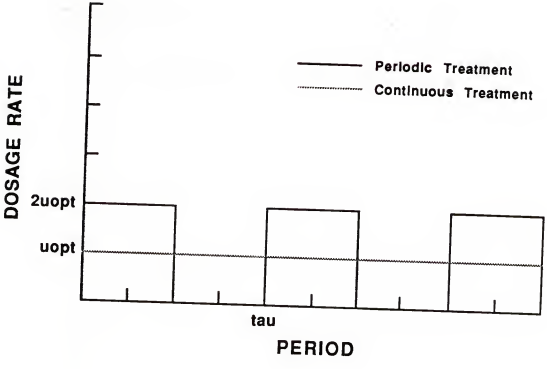

Figure (4-2). Rate of dosage u versus period τ.

$$H = e^{y_n} - qe^{y_c} + \lambda_1 \left(-\alpha y_n - \frac{\gamma_n c}{1 + c}\right) + \lambda_2 \left(- y_c - \frac{\gamma_c c}{1 + c}\right)$$
$$+ \lambda_3 (u - \delta c) + \mu (u - u_{opt}) \qquad (4\text{-}16)$$

λ_i and μ representing Lagrange multipliers for the equality and inequality constraints respectively.

Using this system of equations $\pi(\omega)$ is calculated to be

$$\pi(\omega) = \frac{1}{(\omega^2 + \delta^2)(1 + c^o)^3} \cdot$$

$$\frac{\gamma_n^2 e^{y_n^o}}{(\omega^2 + \alpha^2)(1 + c^o)} - \frac{q\gamma_c^2 e^{y_c^o}}{(\omega^2 + 1)(1 + c^o)} + \frac{2(\gamma_n e^{y_n^o} - \alpha q \gamma_c e^{y_c^o})}{\alpha} \qquad (4\text{-}17)$$

$\pi(\omega)$ is a function of all five dimensionless model parameters. Depending on the choice of those parameters, three regions can be seen (Figures 4-3, 4-4). These regions can be characterized as follows:

Region 1: u_{opt} negative

Region 2: $\pi(\omega)$ positive

Region 3: $\pi(\omega)$ negative

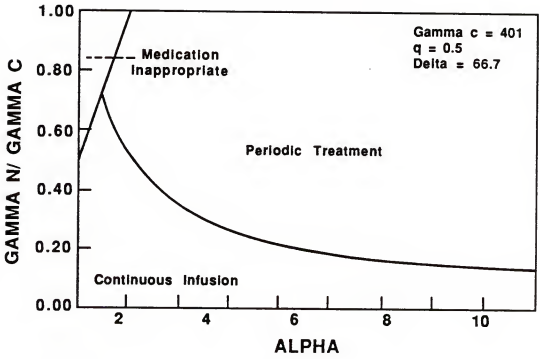

Figure (4-3). The three regions for q=0.5.

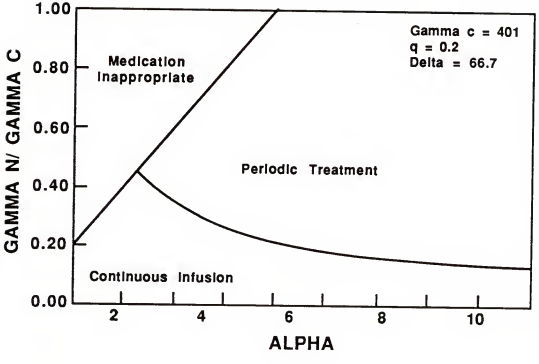

Figure (4-4). The three regions for q=0.2.

For certain values of the five parameters u_{opt}, as given by equation (4-12), is negative. Because J is a monotonic function of u, the optimal dosage for this case is $u_{opt} = 0$. This simply means that the drug chosen is inappropriate and another medication has to be considered whenever the parameters give rise to a point in Region 1.

If they give rise to a point in Region 2 ($\pi(\omega)$ positive), then the model predicts that some form of periodic treatment will be superior to continuous treatment. How to find the optimal length of the treatment period τ as well as the number of days on and off medication will be explained later.

For Region 3, $\pi(\omega)$ is negative which means that continuous treatment (drug given daily, no recovery periods) will render the best results.

To test the effect of the five dimensionless parameters, $\pi(\omega)$ was evaluated numerically and plotted as a function of ω. These results are shown in Figures 4-5 to 4-9. It is seen that $\pi(\omega)$ becomes positive for a range of cycling frequencies, indicating that periodic treatment using these treatment frequencies yields better results than continuous treatment.

From the computation of $\pi(\omega)$ certain important qualitative observations may be made. The length of the treatment cycle is influenced by the growth of tumor cells relative to normal cells (the parameter α), and by the tumor cell kill that the medication causes relative to the kill of benign cells (γ_n, γ_c). An increasing ratio of γ_n/γ_c, which means increasing kill of normal cells compared to malignant ones, requires decreasing cycling frequencies (ω_{opt}). This in turn means longer treatment cycles are necessary to give benign body cells time to

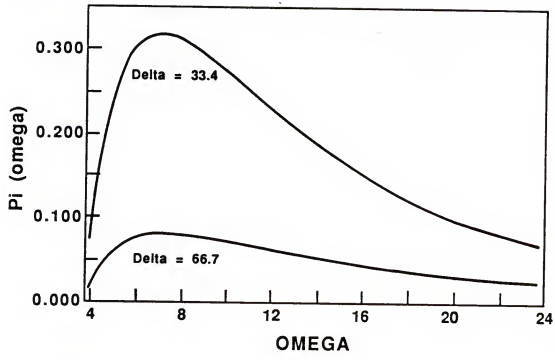

Figure (4-5). The effect of the drug instability δ on $\pi(\omega)$. Model parameters: α=10, γ_c=401, γ_n=320.8, q=0.4

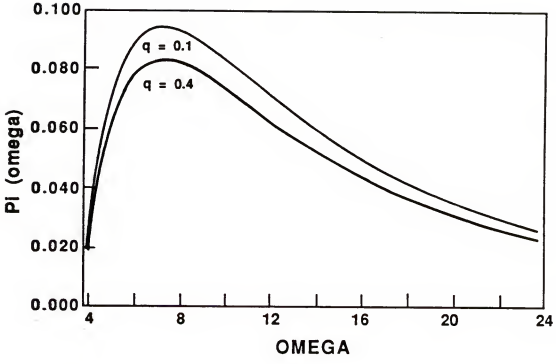

Figure (4-6). The effect of the 'cost variable' q on $\pi(\omega)$. Model parameters: α=10, γ_c=401, γ_n=320.8, δ=66.7

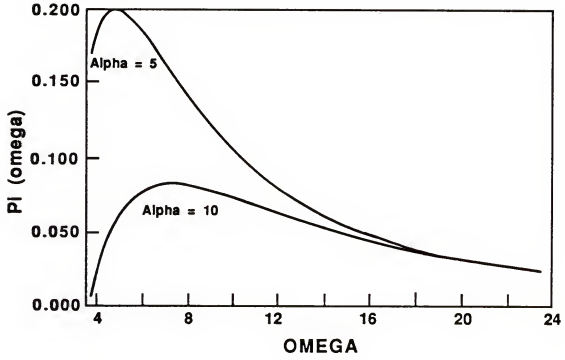

Figure (4-7). The effect of the growth related variable α on $\pi(\omega)$. Model parameters: γ_c=401, γ_n=320.8, δ=66.7, q=0.4

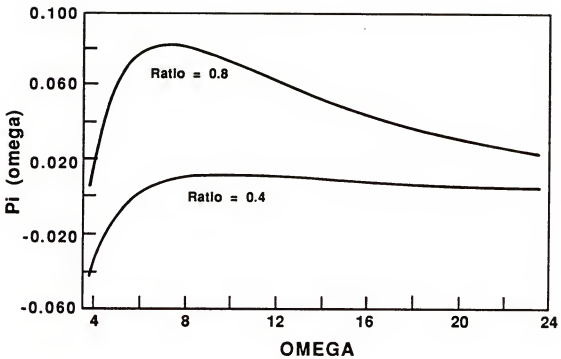

Figure (4-8). The effect of the ratio of γ_n/γ_n on $\pi(\omega)$. Model parameters: α=10, γ_c=401, δ=66.7, q=0.4

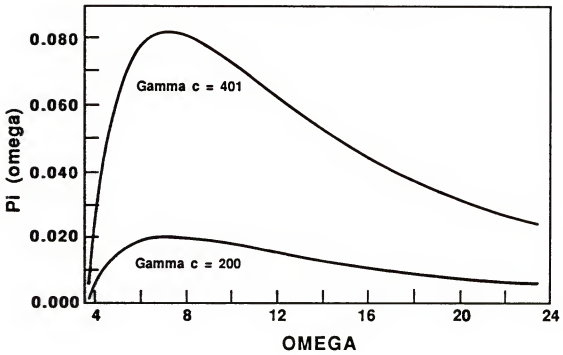

Figure (4-9). The effect of the tumor cell kill variable γ_c or $\pi(\omega)$. Model parameters: α=10, γ_n/γ_c=0.8, δ=66.7, q_c=0.4

recover. The length of the optimal treatment cycle is also influenced by the parameters α and γ_c itself but not in a monotonic fashion. An increasing value of α, which means increasing growth of cancer cells compared to normal cells first causes the optimal treatment frequency to decrease, then to increase again (the value of the extremum is influenced by the other parameters). The same holds true for the parameter γ_c. The parameters which do not influence the length of the treatment cycle are the drug stability (δ) and the "cost parameter" q. It might seem surprising at first that the drug stability influences neither the type of operation (cyclic or continuous as can be seen from equation (4-17)) nor the optimal cycling frequency, but it strongly influences the average amount of drug optimally administered (u_{opt}). This indicates that if a drug is highly unstable it should be given at a higher dosage, if permissible, not in shorter treatment cycles (for this set of growth and kinetic parameters). It is fortunate that the "cost parameter" q, which requires a value judgement by the physician and is not based on physical data, does not influence the length of the treatment cycle.

To verify the predictions of the π-criterion numerical simulations (integrations of equations (4-5) to (4-8) and (4-11) were undertaken. Square wave variations (bang-bang switches) between $u = 2u_{opt}$ and $u = 0$ (see Figure 4-2) were employed, rather than sinusoidal variations, since such type of cycling has previously proven superior and is easier to implement. Figure 4-10 shows plots of the performance measure and the function $\pi(\omega)$ versus the cycling frequency ω. It can be seen that the optimal cycling frequency as obtained by integration (value at which J is maximum) is close to that predicted by the π-criterion (value at which π is maximum).

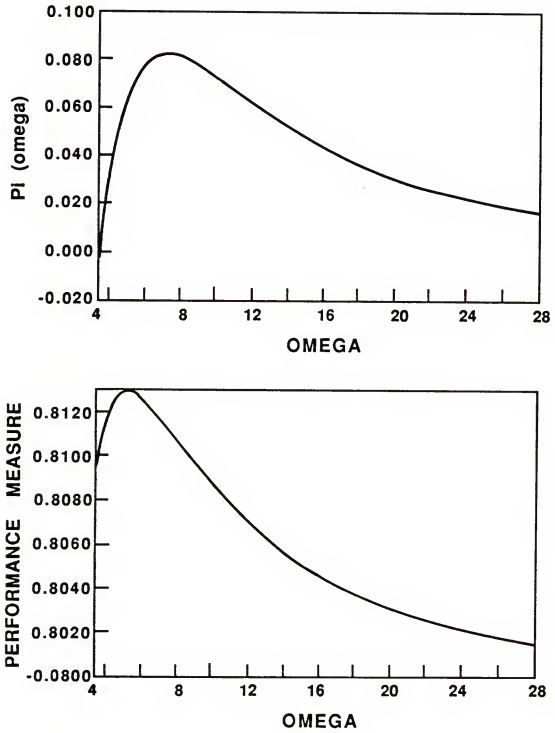

Figure (4-10). $\pi(\omega)$ and the performance measure $J(\omega)$ versus treatment frequency ω. Model parameters as in Figure 4-1.

Although the π-criterion determines the optimal cycling frequency, it does not give any predictions about the optimal wave form, i.e. the optimal fraction of the treatment cycle drug should be administered. Keeping the amount of drug over a period constant, the variable ε is defined as that fraction, while $1-\varepsilon$ is the fraction of the treatment cycle for which the patient stays off medication (Figure 4-11). The numerical simulations show that there exists an optimal ε, as shown in Figure 4-12. An example is given in Appendix H. For a tumor of the given growth characteristics and a drug with the given properties it suggests a treatment cycle of 35 days, 3 of those on medication and 32 off, as well as the optimal rate of dosage. In some cases the optimal fraction ε_{opt} cannot be implemented because the dosage rate u, which is given as the ratio of u_{opt}/ε is limited by u_{max}, the maximum allowable doses according to toxicity criteria. So there is a constraint placed on ε given by

$$\varepsilon_{min} = \frac{u_{opt}}{u_{max}} \tag{4-18}$$

If the calculations yield an ε_{opt} smaller than ε_{min}, then the fraction of the period on medication has to be set at ε_{min}.

Conclusions

The method proposed can help to answer the fundamental questions of treatment strategy for a certain patient and the drug under consideration: (1) Is the drug appropriate? (2) Will continuous or cyclic administration give the best result? (3) How much shall be administered and in which time intervals? The quality of the predictions

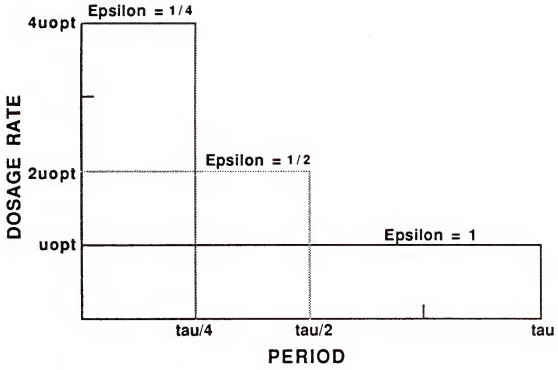

Figure (4-11). Different wave forms, ε=1, 1/2, 1/4.

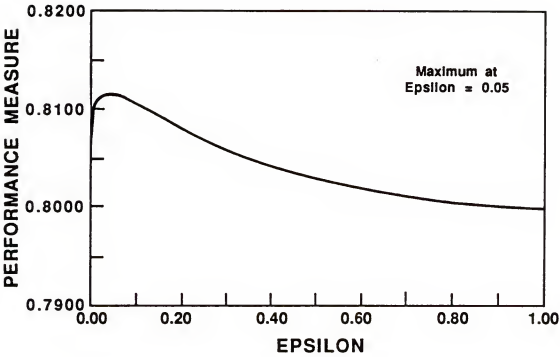

Figure (4-12). The performance measure J versus ε, the fraction of the treatment cycle, a patient receives medication. Model parameters as in Figure 4-4.

depends solely on the quality of the available data. Although the mathematical model used in this paper is rather rudimentary, its predictions are based on the actual patient data. If more is known about the growth history of the tumor and the pharmacokinetics of the drug used, a more sophisticated model can be constructed. The more complete the available data, the better the mathematical model and the better will the predictions about the optimal treatment regimen.

One obvious advantage of a "simplistic" model of the form used in this work is the ease of determination of the model parameters from available data. In addition, the mathematical complexity added by a more sophisticated model can make the determination of the optimal drug administration significantly less tractable. Calculating optimal treatment regimen using even very simplistic models represents an improvement compared to the trial-and-error method still used in clinical practice. Summarizing it shall be stated that the proposed method has proven useful in determining which treatment regimen is optimal for a certain patient and a given drug. It not only clearly separates the regions in which continuous or periodic treatment yields superior results, it also gives, in combination with numerical simulations, the optimal length of the treatment cycle as well as the optimal time on or off the drug and the required dosage.

IV.2. Periodic Impulse Forcing in Cancer Chemotherapy-Determination of the Optimal Treatment Regimen

Introduction

As concluded in the previous Chapter (IV.1.), optimal control theory in general and the π-criterion in particular can make a valuable

contribution in determining how promising a certain treatment approach is. The appropriateness of a drug (combination of drugs) can be established as well as the form of treatment-continuous or periodic. The π-criterion, as explained in Section II.1, was applied to answer the questions stated above.

A point of particular interest is how the body, normal and cancerous cells, reacts to a single injection of drug or a series of injections. An injection of a drug into the body represents an instantaneous addition of a substance to the system and this is to be described mathematically as an impulse. Consequently repeated injections constitute impulse forcing. Impulse forcing is a very common periodic waveform but the predictions of the π-criterion are less reliable here, mainly for two reasons: the π-function strictly predicts improved performance only for sinusoidal waveforms. Square waves, as discussed in the previous chapter, only represent a minor deviation from this waveform. In the case of impulse forcing though, to still administer the same amount of drug over the period in an instantaneous form requires amplitudes which are orders of magnitude higher than those necessary for sinusoidal forcing. For this reason another limitation of the π-criterion becomes important here, the restriction that this method is valid only for small amplitudes. Thus, the π-criterion probably being of very limited use in this case, the only way so far to describe the reaction of a nonlinear system to impulse forcing was numerical integration, point by point, something which is time consuming and tedious.

The problem stated above was a major motivation for the development of the new method presented in Section II.2. "Periodic Impulse Forcing

of Nonlinear Systems." In the following this method will be applied to cancer chemotherapy to investigate the effect of drug injections on normal and malignant cell population, to study the effect of repeated injections, to determine whether steady state or periodic operation is superior, and, whenever applicable, to determine the optimal forcing period.

The Effect of Drug Injections on Normal and Malignant Tissue

Assume a treatment strategy where a drug is injected periodically into the bloodstream. This can be described as a series of impulses which results in an instantaneous addition of a disturbance $\underline{m}$ to the state vector $\underline{y}$ (an instantaneous addition of the dosage u to the plasma drug concentration). The modelling principles remain the same as in the previous chapter. Together with the specific cancerous tissue to be treated, the "limiting tissue"--the most critical one of the normal cell population--will be modelled. Gompertz growth is assumed for both cell types (equation 4-2) as well as saturation effect towards the drug (equation 4-3). Using first order pharmacokinetics (equation 4-4) to relate the drug dosage to the plasma drug concentration and treating the body as one compartment, equations (4-5) to (4-7) adequately describe this system. In dimensionless variables (Appendix G):

$$\frac{dy_n}{dt} = - \alpha y_n - \frac{\gamma_n c}{1 + c} \qquad \text{normal cell population} \qquad (4\text{-}5)$$

$$\frac{dy_c}{dt} = - y_c - \frac{\gamma_c c}{1 + c} \qquad \text{cancer cell population} \qquad (4\text{-}6)$$

$$\frac{dc}{dt} = u - \delta c \qquad \text{drug concentration} \qquad (4\text{-}7)$$

To this three-dimensional system of equations the new method, as introduced in Section II.2., will be applied. Notice that the equations describing the cell populations are independent of each other and both are dependent only on the equation describing the drug instability. Therefore a new, simpler two-dimensional system can be defined

$$\frac{dy_i}{dt} = -\alpha_i y_i - \frac{Y_i c}{1+c} \qquad i = c \text{ or } n \tag{4-19}$$

$$\frac{dc}{dt} = -\delta c \tag{4-20}$$

Equation (4-19) holds true for both the normal cell population ($i = n$ and $\alpha_i = \alpha_c$) and for the malignant population ($i = c$ and $\alpha_i = 1$). Having reduced the three-dimensional system of equations to a two-dimensional one, define now the reduced third order Carleman vector

$$\underline{w} = \begin{pmatrix} x_1 \\ x_2 \\ x_1^2 \\ x_1x_2 \\ x_2^2 \\ x_1^3 \\ x_1^2x_2 \\ \\ x_1x_2^2 \\ x_1^3 \end{pmatrix} = \begin{pmatrix} y_i \\ c \\ y_i^2 \\ y_ic \\ c^2 \\ y_i^3 \\ y_i^2c \\ \\ y_ic^2 \\ c^3 \end{pmatrix} \qquad i = c, n \tag{4-21}$$

This gives rise to the third-order Carleman matrix ($i = c,n$)

$$C_3 = \begin{vmatrix} -\alpha_i & -\gamma_i & 0 & 0 & \gamma_i & 0 & 0 & 0 & -\gamma_i \\ 0 & -\delta & 0 & 0 & 0 & 0 & 0 & 0 & 0 \\ 0 & 0 & -2\alpha_i & -2\gamma_i & 0 & 0 & 0 & 2\gamma_i & 0 \\ 0 & 0 & 0 & -(\alpha_i+\delta) & -\gamma_i & 0 & 0 & 0 & \gamma_i \\ 0 & 0 & 0 & 0 & -2\delta & 0 & 0 & 0 & 0 \\ 0 & 0 & 0 & 0 & 0 & -3\alpha_i & -3\gamma_i & 0 & 0 \\ 0 & 0 & 0 & 0 & 0 & 0 & -(2\alpha_i+\delta) & -2\gamma_i & 0 \\ 0 & 0 & 0 & 0 & 0 & 0 & 0 & -(\alpha_i+2\delta) & 0 \\ 0 & 0 & 0 & 0 & 0 & 0 & 0 & 0 & -3\delta \end{vmatrix} \quad (4\text{-}22)$$

The vector of state variables at the beginning of the period is given by (equation 2-46) which in this case becomes

$$\underline{w}_o = \left[e^{C_3\tau} - \sum_{i=0}^{2} A_i\right]^{-1} \underline{m}^* \quad (4\text{-}23)$$

where

$$\underline{m}^* = \begin{vmatrix} (-\underline{m}) \\ (-m)^{[2]} \\ (-\underline{m})^{[3]} \end{vmatrix} \quad (4\text{-}24)$$

with

$$\underline{m} = \begin{vmatrix} 0 \\ u \end{vmatrix} \quad (4\text{-}25)$$

To administer the same amount of drug over a period as in the case of continuous infusion (steady-state administration) u has to be a function of the forcing period τ.

$$u = \text{dosage rate} \cdot \tau \quad (4\text{-}26)$$

Now define the A_i's. According to equation (2-48)

$$A_o = I_9 \tag{4-27}$$

The reduced forms (after eliminating redundancies in the monomials like x_1x_2 and x_2x_1) of the matrices A_1 and A_2 are as follows:

$$A_1 = \begin{pmatrix} 0 & 0 & 0 & 0 & 0 & 0 & 0 & 0 & 0 \\ 0 & 0 & 0 & 0 & 0 & 0 & 0 & 0 & 0 \\ 0 & 0 & 0 & 0 & 0 & 0 & 0 & 0 & 0 \\ -2u & 0 & 0 & 0 & 0 & 0 & 0 & 0 & 0 \\ 0 & -2u & 0 & 0 & 0 & 0 & 0 & 0 & 0 \\ 0 & 0 & 0 & 0 & 0 & 0 & 0 & 0 & 0 \\ 0 & 0 & -3u & 0 & 0 & 0 & 0 & 0 & 0 \\ 0 & 0 & 0 & -3u & 0 & 0 & 0 & 0 & 0 \\ 0 & 0 & 0 & 0 & -3u & 0 & 0 & 0 & 0 \end{pmatrix} \tag{4-28}$$

$$A_2 = \begin{pmatrix} 0 & 0 & 0 & 0 & 0 & 0 & 0 & 0 & 0 \\ 0 & 0 & 0 & 0 & 0 & 0 & 0 & 0 & 0 \\ 0 & 0 & 0 & 0 & 0 & 0 & 0 & 0 & 0 \\ 0 & 0 & 0 & 0 & 0 & 0 & 0 & 0 & 0 \\ 0 & 0 & 0 & 0 & 0 & 0 & 0 & 0 & 0 \\ 0 & 0 & 0 & 0 & 0 & 0 & 0 & 0 & 0 \\ 0 & 0 & 0 & 0 & 0 & 0 & 0 & 0 & 0 \\ 3u^2 & 0 & 0 & 0 & 0 & 0 & 0 & 0 & 0 \\ 0 & 3u^2 & 0 & 0 & 0 & 0 & 0 & 0 & 0 \end{pmatrix} \tag{4-29}$$

Table 4-1 shows the matrix to be inverted (see equation (4-23)). After inversion it is multiplied by the vector $\underline{m}^*$ to find $\underline{w}$, the vector of state variable at the beginning of a period.

Assume now that the system is subjected to a series of impulses and that all transients have subsided. According to equation (4-2)

$$\dot{\underline{w}} = C_3 \underline{w} \tag{4-30}$$

To observe how the two cell populations react to an injection of drug, equation (4-30) can be solved

$$y_i = g\, e^{C_3 \tau}\, \underline{w}_o \qquad i = c,n \tag{4-31}$$

where

$$g = \begin{vmatrix} 1 \\ 0 \\ 0 \\ 0 \\ 0 \\ 0 \\ 0 \\ 0 \\ 0 \end{vmatrix}^T \tag{4-32}$$

Figure 4-13 shows the reaction of the critical normal and the cancerous cell population to an injection of drug of the optimal steady-state dosage rate ($\tau = 1$). The order of the Carleman approximation used ($\ell = 3$) was found to be very satisfactory since the results obtained with this new method are indistinguishable (for most sets of parameters within four significant figures) from those obtained by numerical integration.

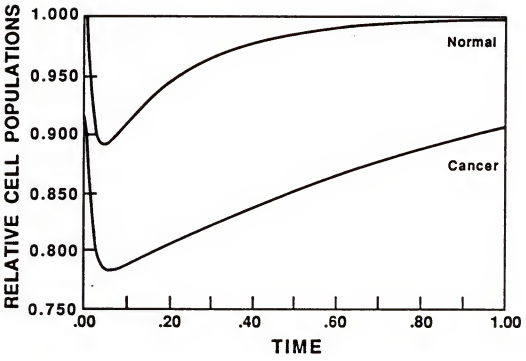

Figure (4-13). The response of normal and malignant cells to a single injection of drug at the steady-state dosage ($\tau = 1$.)

Table 4-1. Listing of All Non-Zero Matrix Elements of $[e^{C_3\tau} - I - A_1 - A_2]$

Matrix element	Value
(1,1)	$e^{-\alpha_i\tau} - 1$
(1,2)	$a(e^{-\delta\tau} - e^{-\alpha_i\tau})$
(1,5)	$b(e^{-2\delta\tau} - e^{-\alpha_i\tau})$
(1,9)	$c(e^{-3\delta\tau} - e^{-\alpha_i\tau})$
(2,2)	$e^{-\delta\tau} - 1$
(3,3)	$e^{-2\alpha_i\tau} - 1$
(3,4)	$2a\,(e^{(-\alpha_i+\delta)\tau} - e^{-2\alpha_i\tau})$
(3,5)	$a^2(e^{-\alpha_i\tau} - e^{-\delta\tau})^2$
(3,8)	$2b(e^{-(\alpha_i+2\delta)\tau} - e^{-2\alpha_i\tau})$
(3,9)	$2ab(e^{-\alpha_i\tau} - e^{-\delta\tau})(e^{-\alpha_i\tau} - e^{-2\delta\tau})$
(4,1)	$2u$
(4,4)	$e^{-(\alpha_i+\delta)\tau} - 1$
(4,5)	$a(e^{-2\delta\tau} - e^{-(\alpha_i+\delta)\tau})$
(4,9)	$b(e^{-3\delta\tau} - e^{-(\alpha_i+\delta)\tau})$
(5,2)	$2u$

Table 4-1 continued

Matrix element	Value
(5,5)	$e^{-2\delta\tau} - 1$
(6,6)	$e^{-3\alpha_i\tau} - 1$
(6,7)	$3a(e^{-(2\alpha_i+\delta)\tau} - e^{-3\alpha_i\tau})$
(6,8)	$3e^{-\alpha_i\tau}[a(e^{-\alpha_i\tau} - e^{-\delta\tau})]^2$
(6,9)	$[-a(e^{-\alpha_i\tau} - e^{-\delta\tau})]^3$
(7,3)	$3u$
(7,7)	$e^{-(2\alpha_i+\delta)\tau}$
(7,8)	$2a(e^{-(\alpha_i+2\delta)\tau} - e^{-(2\alpha_i+\delta)\tau})$
(7,9)	$e^{-\delta\tau}[a(e^{-\alpha_i\tau} - e^{-\delta\tau})]^2$
(8,1)	$-3u^2$
(8,4)	$3u$
(8,8)	$e^{-(\alpha_i+2\delta)\tau} - 1$
(8,9)	$a(e^{-3\delta\tau} - e^{-(\alpha_i+2\delta)\tau})$
(9,2)	$-3u^2$
(9,5)	$3u$
(9,9)	$e^{-3\delta\tau} - 1$

where

$$a = \frac{\gamma_i}{\alpha_i - \delta}$$

$$b = \frac{\gamma_i}{\alpha_i - 2\delta} \qquad i = c,n$$

$$c = \frac{-\gamma_i}{\alpha_i - 3\delta}$$

Optimization of Cancer Chemotherapy

Again, the choice of the proper performance measure is of utmost importance. The ratio of the number of cells at time t of treatment, as represented by $y_i(t)$, divided by the maximum attainable number of cells (without treatment), the performance measure is given by

$$J = \frac{1}{\tau}\int_0^\tau (e^{y_n} - qe^{y_c})dt \tag{4-33}$$

q being the weight factor introduced in the previous chapter. This performance measure has to be expanded into a Taylor series

$$J' = \frac{1}{\tau}\int_0^\tau e^{y_i}\, dt = 1 + \frac{1}{\tau}\int_0^\tau \underline{r}^T\underline{w}\, dt \tag{4-34}$$

where

$$r = \begin{pmatrix} 1 \\ 0 \\ 1/2 \\ 0 \\ 0 \\ 1/6 \\ 0 \\ 0 \\ 0 \end{pmatrix} \tag{4-35}$$

According to equation (2-45)

$$J = 1 + \frac{\underline{r}^T}{\tau} C_3^{-1} [e^{C_3\tau} - I]\underline{W}_o = \\ = 1 + \underline{b}^T \underline{W}_o \qquad (4\text{-}36)$$

Table 4-2: Listing of the elements of

$$\frac{\underline{r}^T}{\tau} C_3^{-1} [e^{C_3\tau} - I]$$

Vector Element	Value
(1)	$-\frac{1}{\alpha_i}(e^{-\alpha_i\tau} - 1)$
(2)	$-\frac{a}{\alpha_i}(e^{-\delta\tau} - e^{-\alpha_i\tau}) + \frac{\gamma_i}{\alpha_i\delta}(e^{-\delta\tau} - 1)$
(3)	$-\frac{1}{4\alpha_i}(e^{-2\alpha_i\tau} - 1)$
(4)	$-\frac{a}{2\alpha_i}(e^{-(\alpha_i+\delta)\tau} - e^{-2\alpha_i\tau}) + \frac{\gamma_i}{2\alpha_i(\alpha_i+\delta)}(e^{-(\alpha_i+\delta)\tau} - 1)$
(5)	$-\frac{b}{\alpha_i}(e^{-2\delta\tau} - e^{-\alpha_i\tau}) - \frac{a^2}{4\alpha_i}(e^{-\alpha_i\tau} - e^{-\delta\tau})^2 + \frac{\gamma_i a}{2\alpha_i(\alpha_i+\delta)}(e^{-2\delta\tau} - e^{-(\alpha_i+\delta)\tau}) - \frac{\gamma_i}{2\alpha_i\delta}(1 + \frac{\gamma_i}{2(\alpha_i+\delta)})(e^{-2\delta\tau} - 1)$

Table 4-2 continued

Vector Element	Value
(6)	$-\frac{1}{18\alpha_i}(e^{-3\alpha_i\tau} - 1)$
(7)	$-\frac{a}{6\alpha_i}(e^{-(2\alpha_i+\delta)\tau} - e^{-3\alpha_i\tau}) + \frac{\gamma_i}{6\alpha_i(2\alpha_i+\delta)}(e^{-(2\alpha_i+\delta)\tau} - 1)$
(8)	$-\frac{b}{2\alpha_i}(e^{-(\alpha_i+2\delta)\tau} - e^{-2\alpha_i\tau}) - \frac{3e^{-\alpha_i\tau}[a(e^{-\alpha_i\tau} - e^{-\delta\tau})]^2}{18\alpha}$ $+\frac{a\gamma_i d}{3\alpha_i}(e^{-(\alpha_i+2\delta)\tau} - e^{-(2\alpha_i+\delta)\tau}) -$ $-\frac{\gamma_i}{(\alpha_i+2\delta)\alpha_i}(\frac{1}{2} + \frac{\gamma_i d}{3})(e^{-(\alpha_i+2\delta)\tau} - 1)$
(9)	$-\frac{c}{\alpha_i}(e^{-3\delta\tau} - e^{-\alpha_i\tau}) - \frac{ab}{2\alpha_i}(e^{-\alpha_i\tau} - e^{-\delta\tau})(e^{-\alpha_i\tau} - e^{-2\delta\tau}) +$ $\frac{\gamma_i b}{2\alpha_i(\alpha_i+\delta)}(e^{-3\delta\tau} - e^{-(\alpha_i+\delta)\tau})$ $-\frac{[a(e^{-\alpha_i\tau} - e^{-\delta\tau})]^3}{18\alpha_i} + \frac{\gamma_i e^{-\delta\tau}}{6\alpha_i(2\alpha_i+\delta)}[a(e^{-\alpha_i\tau} - e^{-\delta\tau})]^2$ $-\frac{\gamma_i a}{(\alpha_i+2\delta)\alpha_i}(\frac{1}{2} + \frac{\gamma_i}{3(2\alpha_i+\delta)}(e^{-3\delta\tau} - e^{-(\alpha_i+2\delta)\tau})$ $+\frac{\gamma_i}{3\alpha_i\delta}[1 + \frac{\gamma_i}{2}(\frac{1}{\alpha_i+2\delta} + \frac{1}{\alpha+\delta}) + \frac{\gamma_i^2}{3(2\alpha_i+\delta)(\alpha_i+2\delta)}(e^{-3\delta\tau} - 1)$

a, b, c are as defined in Table 4-1.

Figure 4-14 shows that for $\gamma_n = 350$, $\gamma_c = 401$, $\delta = 6.67$, $\alpha = 5$, $q = .2$ periodic treatment indeed does yield better results than continuous treatment as expected from the π-criterion. Furthermore it is obvious that the new method used in this chapter is in excellent agreement with the mathematical simulations (integrations) in predicting the optimal length of the treatment cycle ($\tau_{opt} = 2.2$) while the predictions of the π-criterion are less accurate in this case ($\tau_{opt} = 1.6$).

For a different set of parameters however, ($\gamma_n = 240$, $\gamma_c = 401$, $\delta = 66.7$, $\alpha = 8$, $q = .5$) the new method fails to predict the optimal treatment frequency. It still yields the vector $\underline{w}_o$, the cell populations at the beginning of each treatment cycle with highest accuracy, but in this case the treatment is so successful that $|y_c| > 1$. This of course means that the Taylor series expansion used in the performance measure is no longer valid and thus the optimal length of the treatment cycle cannot be predicted. However in this case the π-criterion succeeds in predicting the optimal period ($\tau_{opt} = 0.87$ versus 0.85 obtained by integration).

The new method has particular value for all those cases, where the π-criterion is inapplicable because it does not require (like the π-criterion does) that the performance measure J exhibits a maximum with respect to the control variable u. If instead of the performance measure (4-33) one chooses to maximize the ratio of the relative cell populations, as might be indicated for some types of cancer, a linear performance measure arises.

$$J = \frac{1}{\tau}\int_0^{\tau} \left(\ln \frac{x_n/x_{n,\infty}}{x_c/x_{c,\infty}}\right)dt = \frac{1}{\tau}\int_0^{\tau} (y_1 - y_2)dt \qquad (4\text{-}37)$$

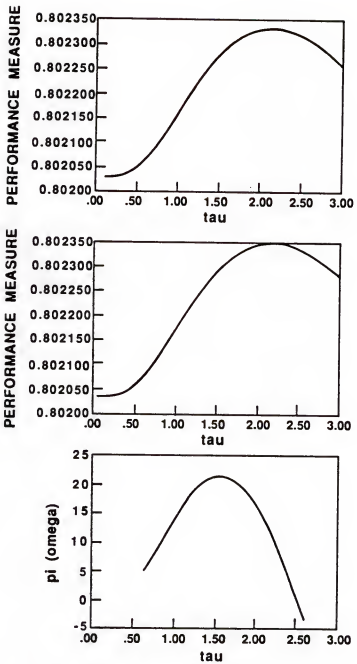

Figure (4-14). The prediction of the optimal cycling period by: a) numerical integration
b) the new method
c) the π-criterion

No optimal steady-state value exists for the control variable and therefore the π-criterion, which compares periodic operation to the optimal steady-state operation, cannot be applied. For the performance measure as defined by equation (4-38)

$$J = \frac{1}{\tau}\int_0^{\tau} \underline{r}^T \underline{w}\, dt = \frac{\underline{r}^T}{\tau} C_3^{-1}[e^{C_3\tau} - I]\, \underline{w}_o = \underline{b}^T \underline{w}_o \tag{4-38}$$

where $\underline{r}$ is given by

$$\underline{r} = \begin{vmatrix} 1 \\ 0 \\ 0 \\ 0 \\ 0 \\ 0 \\ 0 \\ 0 \\ 0 \end{vmatrix} \tag{4-39}$$

In this case the vector $\underline{b}$ in equation (4-38) is given by

$$\begin{vmatrix} -\frac{1}{\alpha_i}(e^{-\alpha_i\tau} - 1) \\ -\frac{a}{\alpha_i}(e^{-\delta\tau} - e^{-\alpha_i\tau}) + \frac{\gamma_i}{\alpha_i\delta}(e^{-\delta\tau} - 1) \\ 0 \\ 0 \\ -\frac{b}{\alpha_i}(e^{-2\delta\tau} - e^{-\alpha_i\tau}) - \frac{\gamma_i}{2\alpha_i\delta}(e^{-2\delta\tau} - 1) \\ 0 \\ 0 \\ 0 \\ -\frac{c}{\alpha_i}(e^{-3\delta\tau} - e^{-\alpha_i\tau}) + \frac{\gamma_i}{3\alpha_i\delta}(e^{-3\delta\tau} - 1) \end{vmatrix} \tag{4-40}$$

Figure 4-15 shows the dependence of the linear performance measure J on the cycling period τ for a certain set of parameters ($Y_n = 240$, $Y_c = 401$, $\delta = 66.7$, $\alpha = 8$, $q = 5$). Three dosages were investigated, and the results show clearly, that continuous infusion (steady-state treatment) is superior to any kind of periodic regimen. The higher the dosage, the higher is the performance measure. The optimal dosage rate therefore is the highest one allowed by toxicity criteria. In most cases continuous treatment is rather inconvenient, because it may force the patient to stay in the hospital for an extended amount of time. Alternatively, if this form of schedule is not possible, the treatment cycles should be kept as short and as frequent as possible and the dosage the highest possible one.

Conclusions

In the case of impulse forcing, because of the strong deviation from the sinusoidal wave form and the high amplitudes necessary, the π-criterion does not always succeed in predicting the optimal length of the treatment cycle. The new method, on the other hand, is capable of predicting the optimal treatment strategy accurately, as long as the state variables are defined in such a way that they remain in the range where the Taylor Series expansion is valid.

For a performance measure which maximizes the difference in the cell populations, weighed by a weighing factor, a periodic schedule is superior to continuous treatment and an optimal cycle-length can be found. When a linear performance measure is employed, continuous treatment is preferable. If this is not possible, the treatment cycles should be kept as short and the dosage rates as high as possible.

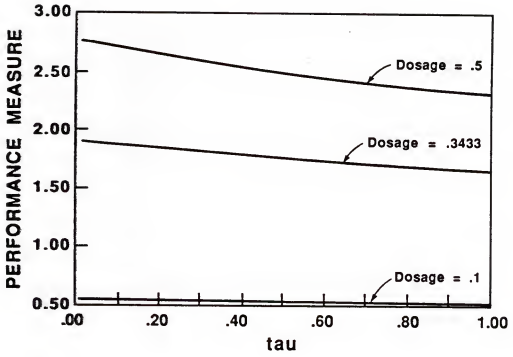

Figure (4-15). The effect of the dosage on the (linear) performance measure

CHAPTER V
SUMMARY AND CONCLUSIONS

Over the past few years it has been realized that periodic operation of biochemical reactors can be superior to steady-state operation. Although some workers had tried to assess the effect experimentally in the past, no systematical investigation of the effect of periodic operation had ever been undertaken.

In a very different scientific field, cancer chemotherapy, it had been disputed for many years whether cyclic or continuous treatment of cancer will yield better results. In this dissertation the attempt has been made to answer some of these questions.

There are two possible approaches to determining the optimal periodic conditions: an ad hoc trial-and-error procedure or a systematical search utilizing mathematical modeling as a guidance tool. Based on mathematical process models, methods of optimal control theory can be applied to answer the question of what the optimal period, amplitude and wave form are.

Among the already established methods perhaps the most well known is the π-criterion. It has proven useful in many cases for finding the optimal periodic operating conditions, but does not perform quite as well in cases where the wave form deviates strongly from a sinusoid or where amplitudes are too high.

For this reason a new method "periodic impulse forcing of nonlinear systems" has been introduced in this dissertation specifically for the study of periodic impulse forcing.

The π-criterion was applied to predict optimal periodic conditions for a chemostat undergoing square wave forcing in the dilution rate. It was concluded that enhanced productivity of biomass can result for certain cycling frequencies. This is a consequence of the fact that there is a time-lag in the culture adaptation to the new growth rate when a disturbance in introduced. The predictions obtained with methods of optimal control theory can serve as a guide for finding the actual experimental operating conditions, which maximize the performance measure. In order to be able to describe the experimental results qualitatively it was indeed necessary to include a time-lag in the unstructured model describing the response to a step change in the dilution rate. It was found that for a step down the culture continues to grow according to the initial growth rate for a certain time, while when the dilution rate was stepped up, growth even stalled during this lag-time.

The same effects were observed when the system was subjected to square wave variations in the dilution rate. A considerable improvement in the reactor performance was obtained for a cycling frequency of three hours. A possible explanation for this phenomenon is that in this case, a high (exponential) growth rate coincides with a high concentration of biomass at a time when there is ample substrate present.

Just as the growth of cells in a reactor can be maximized by a certain "feeding schedule," the growth of unwanted cells, i.e. cancer cells, can be minimized by a certain treatment schedule. The limiting

factor in cancer chemotherapy is the toxicity of the drug to the normal, homeostatically controlled, cell population. Thus, an optimization problem exists between killing the maximum number of cancer cells while doing as little damage as possible to the benign cell population.

The π-criterion helped in finding an answer to the following questions: (1) Is the drug appropriate? (2) Will continuous or cyclic administration give better results? (3) How much shall be administered and in which time intervals? Although the mathematical model used was rather rudimentary, it was based on actual patient data and the resulting optimal treatment schedule is among those used in clinical practice.

If the point of interest is the reaction of normal and malignant cells to a single injection of drug or a series of injections, the predictions of the π-criterion were found to be less accurate because some of its limitations became relevant in this case. This was a major motivation for the development of the new method "periodic impulse forcing of nonlinear systems." This method has been found to be very successful in predicting the optimal periodic conditions, as long as the state variables are defined in such a way that they remian in the range, where the Taylor Series expansion is valid.

The quality of any prediction made by methods of optimal control theory depends to a great extent on the quality of the mathematical model used to describe the system in question. This in turn depends on the quality of the experimental/patient data. The more complete the available data, the better is the mathematical model and the better are the predictions about the optimal periodic operating conditions. Therefore, in optimizing any process it frequently is worth the effort

to conduct experiments designed especially to obtain the best possible dynamic model in an effort to obtain predictions, which are not only qualitatively true, but also quantitatively good.

APPENDIX A
OPTIMAL PERIODIC SQUARE WAVE FORCING:
A NEW METHOD (LYBERATOS AND SVORONOS [24])

Consider a process described by

$$\dot{\underline{x}} = \underline{F}(\underline{x},u); \quad \underline{F}(0,0) = 0 \tag{A-1}$$

where $\underline{F}(\underline{x}, u)$ is analytic in $\underline{x}$ at $\underline{0}$ for all values of u in the admissible range. $\underline{x}$ and u are the state vector and scalar input deviations from their optimal steady-state, respectively. The objective is to find the periodic pulse input described by

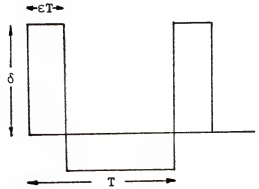

$$u = \begin{cases} \sigma & t\varepsilon\ [nT, (n+\varepsilon)T] \\ \rho = \dfrac{\varepsilon\delta}{\varepsilon-1} & t\varepsilon\ [(n+\varepsilon)T, (n+1)T] \end{cases} \tag{A-2}$$

that maximizes the time-averaged performance measure

$$J = \frac{1}{T} \int_0^T P(\underline{x}, u)dt \tag{A-3}$$

which, in Carleman coordinates, takes the form

$$J = \frac{1}{T} \quad [r_o(u) + \underline{r}^T(u)\underline{w}(t)]dt \tag{A-4}$$

$\underline{w}(t)$ being the state vector (in Carleman coordinates) as introduced in Chapter II.

Theorem: The performance measure is given by

$$\begin{aligned} J(T, \varepsilon, \delta) = &[\underline{r}^T(\rho)\ S(\rho)^{-1} - \underline{r}^T(\delta)\ S(\delta)^{-1}].\frac{(I-R)(I-DR)^{-1}(I-D)}{T}. \\ &\cdot[S(\rho)^{-1}\underline{z}(\rho) - S(\delta)^{-1}\underline{z}(\delta)] \\ &+ \varepsilon[\underline{r}^T(\rho)\ S(\rho)^{-1}\underline{z}(\rho) - \underline{r}^T(\delta)\ S(\delta)^{-1}\underline{z}(\delta)] \\ &- \underline{r}^T(\rho)\ S(\rho)^{-1}\underline{z}(\rho) + r_o(\delta)\varepsilon + r_o(\rho)(1-\varepsilon) \end{aligned} \tag{A-5}$$

where $R = \exp\ [S(\rho)(1-\varepsilon)T]$ and

$D = \exp\ [S(\delta)\varepsilon T]$

and $S(\cdot)$ is the Carleman matrix.

APPENDIX B
DERIVATION OF THE MATRICES A_i
(CHAPTER II.2.)

This appendix will illustrate more explicitly how equation (2-49) has to be used. In the following the matrices A_0 - A_{j-1} will be derived for an n-dimensional system and the 4th order of the Carleman approximation (ℓ=4)

by definition: $A_0 = I$

$$A_i = \begin{pmatrix} \underline{0}_{n \times n} & \cdots & \cdots & \underline{0}_{n \times n^{\ell}} \\ \vdots & & & \vdots \\ \underline{0}_{n^i \times n} & & & \\ \Sigma^* I \otimes (-\underline{m})^{[i]} & \ddots & & \\ \vdots & & \ddots & \\ \underline{0}_{n^{\ell} \times n} & \cdots & \Sigma^* I^{[\ell-i]} \otimes (-\underline{m})^{[i]} \; \underline{0}_{n^{\ell} \times n^{\ell-i+1}} & \underline{0}_{n^{\ell} \times n^{\ell}} \end{pmatrix}$$

therefore

$$A_1 = \begin{pmatrix} \underline{0}_{n \times n} & \underline{0}_{n \times n^2} & \underline{0}_{n \times n^3} & \underline{0}_{n \times n^4} \\ \Sigma^* I \circledast (-\underline{m}) & \underline{0}_{n^2 \times n^2} & \underline{0}_{n^2 \times n^3} & \underline{0}_{n^2 \times n^4} \\ \underline{0}_{n^3 \times n} & \Sigma^* I^{[2]} \circledast (-\underline{m}) & \underline{0}_{n^3 \times n^3} & \underline{0}_{n^3 \times n^4} \\ \underline{0}_{n^4 \times n} & \underline{0}_{n^4 \times n^2} & \Sigma^* I^{[3]} \circledast (-\underline{m}) & \underline{0}_{n^4 \times n^4} \end{pmatrix}$$

$$A_2 = \begin{pmatrix} \underline{0}_{n \times n} & \underline{0}_{n \times n^2} & \underline{0}_{n \times n^3} & \underline{0}_{n \times n^4} \\ \underline{0}_{n^2 \times n} & \underline{0}_{n^2 \times n^2} & \underline{0}_{n^2 \times n^3} & \underline{0}_{n^2 \times n^4} \\ \Sigma^* I \circledast (-\underline{m})^{[2]} & \underline{0}_{n^3 \times n^2} & \underline{0}_{n^3 \times n^3} & \underline{0}_{n^3 \times n^4} \\ \underline{0}_{n^4 \times n} & \Sigma^* I^{[2]} \circledast (-\underline{m})^{[2]} & \underline{0}_{n^4 \times n^3} & \underline{0}_{n^4 \times n^4} \end{pmatrix}$$

$$A_3 = \begin{pmatrix} \underline{0}_{n \times n} & \underline{0}_{n \times n^2} & \underline{0}_{n \times n^3} & \underline{0}_{n \times n^4} \\ \underline{0}_{n^2 \times n} & \underline{0}_{n^2 \times n^2} & \underline{0}_{n^2 \times n^3} & \underline{0}_{n^2 \times n^4} \\ \underline{0}_{n^3 \times n} & \underline{0}_{n^3 \times n^2} & \underline{0}_{n^3 \times n^3} & \underline{0}_{n^3 \times n^4} \\ \Sigma^* I \circledast (-\underline{m})^{[3]} & \underline{0}_{n^4 \times n^2} & \underline{0}_{n^4 \times n^3} & \underline{0}_{n^4 \times n^4} \end{pmatrix}$$

A_i always is a square matrix with the dimensions of $\sum_{k=1}^{i} n^k$.

APPENDIX C
DERIVATION OF RESULTS IN TABLE (2-1)

This appendix will illustrate how the results in Table 2-1 were obtained. They will be derived for the third-order Carleman approximation. In dimensionless variables, the system described by eq. (2-56) around $\bar{x}=1$ is

$$\dot{x} = - x - x^2 \tag{C-1}$$

The third-order Carleman vector is defined as

$$\underline{w}_o = \begin{vmatrix} x_1 \\ x_2 \\ x_3 \end{vmatrix} = \begin{vmatrix} x_1 \\ x_1^{[2]} \\ x_1^{[3]} \end{vmatrix} \tag{C-2}$$

$$\begin{aligned} \dot{x}_1 &= - x_1 - x_2 \\ \dot{x}_2 &= 2x_2 - 2x_3 \\ \dot{x}_3 &= - 3x_3 \end{aligned}$$

(only terms up to 3rd order were retained)

Therefore,

$$C_\ell = C_3 = \begin{vmatrix} -1 & -1 & 0 \\ 0 & -2 & -2 \\ 0 & 0 & -3 \end{vmatrix} \tag{C-3}$$

From eq. (2-41)

$$\underline{w}_o = [e^{C_3\tau} - \sum_{i=0}^{2} A_i]^{-1} \underline{m}^* \tag{C-4}$$

where

$$A_1 = \begin{vmatrix} 0 & 0 & 0 \\ -2m & 0 & 0 \\ 0 & -3m & 0 \end{vmatrix} \quad \text{and} \tag{C-5}$$

$$A_2 = \begin{vmatrix} 0 & 0 & 0 \\ 0 & 0 & 0 \\ 3m^2 & 0 & 0 \end{vmatrix} \tag{C-6}$$

so

$$\underline{w}_{o_2} = [e^{C_3\tau} - I - A_1 - A_2]^{-1} \underline{m}^* \tag{C-7}$$

$$e^{C_3\tau} = \begin{vmatrix} e^{-\tau} & e^{-2\tau} - e^{-\tau} & e^{-3\tau} - 2e^{-2\tau} + e^{-\tau} \\ 0 & e^{-2\tau} & 2e^{-3\tau} - 2e^{-2\tau} \\ 0 & 0 & e^{-3\tau} \end{vmatrix} \tag{C-8}$$

Therefore the matrix to invert is

$$E = \begin{vmatrix} e^{-\tau} - 1 & e^{-2\tau} - e^{-\tau} & e^{-3\tau} - 2e^{-2\tau} + e^{-\tau} \\ 2m & e^{-2\tau} - 1 & 2e^{-3\tau} - 2e^{-2\tau} \\ -3m^2 & 3m & e^{-3\tau} - 1 \end{vmatrix} \tag{C-9}$$

For small values of τ the matrix E may become nearly singular, which can lead to numerical errors during inversion. In this case matrix E needs to be evaluated and inverted numerically, and numerically multiplied by the vector $\underline{m}^*$.

$$\underline{w}_o = E^{-1} \cdot \underline{m}^* \tag{C-10}$$

where

$$\underline{m}^* = \begin{vmatrix} (-m) \\ (-m)^{[2]} \\ (-m)^{[3]} \end{vmatrix} \tag{C-11}$$

This can be done using a maximum pivot strategy. The performance measure is given by

$$J = \frac{\underline{r}^T}{\tau} C_3^{-1} \left[e^{C_3 \tau} - I \right] \underline{w}_o \tag{C-12}$$

where

$$r = \begin{vmatrix} 1 \\ 0 \\ 0 \end{vmatrix} \tag{C-13}$$

Combining eq. (C-10) and (C-11) or (C-12) an (C-13), respectively, leads to the results in Table 2-1.

APPENDIX D

$\pi(\omega)$ FOR A MONOD MODEL WITH DELAY AS GIVEN BY EQUATIONS (3-11) - (3-13)

$$\pi(\omega) = \frac{2}{M}\{\omega^4 F^2 G^3 + \omega^2 FG(\hat{D}^2 FG\hat{K}_s + \hat{D}F^2G^2\hat{K}_s + \hat{D}^2FG^2 - \hat{D}G\hat{\alpha}^2 + \hat{D}FG\hat{K}_s\hat{\alpha}$$

$$- FG\hat{K}_s\hat{\alpha}^2) - \hat{D}^2FG^2\hat{\alpha}^2(\hat{D} + F\hat{K}_s)\}$$

where

$$M = \omega^6 F^2\hat{K}_s^2 + \omega^4 F^2\hat{K}_s^2\,[(\hat{\alpha}+\hat{D}+FG)^2 - 2\hat{\alpha}(\hat{D}+FG)]$$

$$+ \omega^2 F^2\hat{K}_s^2\hat{\alpha}[\hat{\alpha}(\hat{D}+FG)^2 - 2\hat{D}FG(\hat{\alpha}+\hat{D}+FG)]$$

$$+ \hat{D}^2F^4G^2\hat{K}_s^2\hat{\alpha}^2$$

$$F = \frac{1-\hat{D}}{\hat{K}_s} \qquad \text{and}$$

$$G = 1-\hat{D}-\hat{D}\hat{K}_s$$

In the above $\hat{D}$ is the optimum steady-state dilution rate.

APPENDIX E

$\pi(\omega)$ FOR MONOD MODEL WITH DELAY AS GIVEN BY EQUATIONS (3-11), (3-12) AND (3-21)

$$\pi(\omega) = \frac{4D^2 - 4D^2\cos(\omega\tau)\mu_m^2 K_s^2 x^3}{ADY^2F^4} -$$

$$\frac{2E\mu_m K_s x^2\omega^2\cos\omega\tau}{ADYF^2}$$

$$+ \frac{[2D-4D\cos(\omega\tau)]D\mu_m K_s x^2}{AYF^2} + \frac{2DK_s\mu_m x^2\omega\sin(\omega\tau)}{AYF^2}$$

$$- \frac{2Dx^2(D^2 + \omega^2)}{AYF}$$

where $F = K_s + s$,

$$s = \frac{K_s D}{\mu_m - D} \quad , \qquad x = Y(S^\circ - s)$$

and

$$A = \left(\frac{DK_s\mu_m x\cos(\omega\tau)}{YF^2} - \omega^2 \right)^2 + \left(\frac{K_s\mu_m x\omega}{YF^2} + D\omega - \frac{DK_s\mu_m x\sin(\omega\tau)}{YF^2} \right)^2$$

In the above D is the optimal steady-state dilution rate.

APPENDIX F
$\pi(\omega)$ FOR THE WILLIAMS MODEL

$$\pi(\omega) = \frac{1}{M}\left[-32\omega^4\tilde{\alpha}^2(1+\tilde{\alpha})^3 + 8\omega^2(4\tilde{\alpha}^5 + 16\tilde{\alpha}^4 + 24\tilde{\alpha}^3 + 18\tilde{\alpha}^2 + 7\tilde{\alpha} + 1)\right.$$

$$\left. + 8\tilde{\alpha}^3 + 16\tilde{\alpha}^2 + 10\tilde{\alpha} + 2\right]$$

where

$$M = (-4\omega^2\tilde{\alpha}^2 + 1) \cdot \left[[(1 + 2\tilde{\alpha}) - 4(1 + \tilde{\alpha})^2\omega^2]^2 + 16(1+\tilde{\alpha})^4\omega^2\right]$$

APPENDIX G
DERIVATION OF THE DIMENSIONLESS MODEL FOR
CANCER CHEMOTHERAPY (EQUATIONS (4-5) TO ((4-8))

Given the Gompertz equation:

$$\frac{d\ell n\hat{x}_i}{dt} = A_o - \alpha_i \ell n \frac{\hat{x}_i}{\hat{x}_{i,o}} \tag{G-1}$$

defining

$$A_o = \alpha_i \ell n \frac{\hat{x}_{i,\infty}}{\hat{x}_{i,o}} \tag{G-2}$$

Substituting (A2) into (A1)

$$\frac{d\hat{x}_i}{dt} = - x_i \alpha_i \ell n \frac{\hat{x}_i}{\hat{x}_{i,\infty}} \tag{G-3}$$

defining dimensionless variables as follows:

$$y_n = \ell n \frac{x_n}{x_{n,\infty}} \qquad \gamma_n = \frac{k_n}{\alpha_c} \qquad e = \frac{\hat{c}}{k}$$

$$y_c = \ell n \frac{x_c}{x_{c,\infty}} \qquad \gamma_c = \frac{k_c}{\alpha_c} \qquad u = \frac{\hat{u}}{\alpha_c k}$$

$$t = \alpha_c \hat{t} \qquad \alpha = \frac{\alpha_n}{\alpha_c} \qquad \delta = \frac{\hat{\delta}}{\alpha_c}$$

and substituting into (G-4 - G-6)

$$\frac{dx_n}{d\hat{t}} = - \alpha_n x_n \ell n \frac{x_n}{x_{n,\infty}} - \frac{k_n \hat{c}}{k + \hat{c}} x_n \tag{G-4}$$

$$\frac{dx_c}{d\hat{t}} = - \alpha_c x_c \ell n \frac{x_c}{x_{c,\infty}} - \frac{k_c \hat{c}}{k + \hat{c}} x_c \tag{G-5}$$

$$\frac{d\hat{c}}{d\hat{t}} = \hat{u} - \hat{\delta c} \tag{G-6}$$

gives the dimensionless model

$$\frac{dy_n}{dt} = - \alpha y_n - \frac{\gamma_c c}{1 + c} \tag{G-7}$$

$$\frac{dy_c}{dt} = - y_c - \frac{\gamma_c c}{1 + c} \tag{G-8}$$

$$\frac{dc}{dt} = u - \delta c \qquad (G\text{-}9)$$

APPENDIX H
CALCULATION OF THE OPTIMAL TREATMENT PROTOCOL FOR CANCER CHEMOTHERAPY (CHAPTER IV)

Keeping the total amount of drug constant over the length of a treatment cycle, ε is defined as the fraction of the cycle the patient receives a drug (Fig. 4-11).

The dosage ω given during this period is u_{opt}/ε (so that equation (4-15) is satisfied). For small values of ε, u might become higher than the highest physiological allowable dosage u_{max}. Then $u = u_{max}$ and $\varepsilon_{min} = \frac{u_{opt}}{u_{max}}$.

An example shall illustrate this method: For the following parameter choices:

$\alpha = 15$ $\quad Y_c = 401$ $\quad q = 0.4$

$\delta = 66.7$ $\quad Y_n = 160$

the π-criterion yields an optimal treatment cycle of 35 days. Numerical integrations show that $\varepsilon_{opt} = 0.08$ which translates into 3 days of treatment and 32 days without medication.

REFERENCES

1. CONSTANTINIDES, A., SPENCER, J.L. and Gaden, E.C., 1970, Biotechnol. Bioeng., 12, 1081.

2. HO, L.Y. and HUMPHREY, A.E., 1970, Biotechnol. Bioeng., 12, 291.

3. GUTHKE, R. and KNORRE, W.A., 1981, Biotechnol. Bioeng., 23, 2771.

4. OHNO, H., NAKANISHI, E. and TAKAMATSU, T., 1976, Biotechnol. Bioeng., 18, 847.

5. CIFTCI, T., CONSTANTINIDES, A. and WANG, S.S., 1983, Biotechnol. Bioeng., 25, 2007.

6. STANISKIS, J. and LIVISAUSKAS, D., 1983, Biotechnol. Bioeng., 25, 985.

7. PARK, S.H., LEE, S.B. and RYU, D.D.Y., 1981, Biotechnol. Bioeng., 23, 1237.

8. BAILEY, J.E., HORN, F.J.H. and LIN, R.C., 1971, AIChE J., 17, 818.

9. YEUNG, S.Y.S., SINCIK, D. and BAILEY, J.E., 1980, Water Research, 14, 77.

10. DOUGLAS, J.M., 1967, I&EC Proc. Des. and Dev., 6, 43.

11. HORN, F.J.H. and LIN, R.C., 1967, I&EC Proc. Des. and Dev., 6, 21.

12. BAILEY, J.E., 1972, Int. J. of Control, 16, 311.

13. BAILEY, J.E. and HORN, F.J.H., 1971, J. Optim. Theory Applic., 7, 378.

14. BAILEY, J.E., 1974, Chem. Eng. Commun., 1, 111.

15. PICKET, A.M., BAZIN, M.J. and TOPIWALI, H.H., 1980, Biotechnol. Bioeng., 22, 1213.

16. BORZANI, W., GREGORI, R.E. and VAIRO, M.C.R., 1976, Biotechnol. Bioeng., 18, 623.

17. PICKET, A.M., BAZIN, M.J. and TOPIWALA, H.H., 1979, Biotechnol. Bioeng., 21, 1043.

18. VAIRO, M.L.R., BORZANI, W. and MAGALHAES, P., 1977, Biotechnol. Bioeng., 19, 595.

19. ZINES, D.O. and ROGERS, P.L., 1971, Biotechnol. Bioeng., 13, 293.

20. WELLES, J.B. and BLANCH, H.W., 1976, Biotechnol. Bioeng., 18, 129.

21. KIRK, D.E., 1970, Optimal Control Theory (Englewood Cliffs, New Jersey: Prentice-Hall, Inc.).

22. BITTANTI, S., FRONZA, G. and GUARDABASSI, G., 1973, IEEE Trans. on Automatic Control, AC-18, 33.

23. SINCIK, D. and BAILEY, J.E., 1978, Int. J. of Control, 27, 547.

24. LYBERATOS, G. and SVORONOS, S.A., Proceedings American Control Conference, Minneapolis, June 1987.

25. CARLEMAN, T., 1932, Acta Math., 59, 63.

26. BELLMAN, R. and RICHARDSON, J.M., 1963, Quart. Appl. Math., 20, 333.

27. MONTROLL, E.W. and HELLEMAN, R.H.G., 1976, AIP Confer. Proc. 27, 75.

28. SVORONOS, S., STEPHANOPOULOS, G. and ARIS, R., 1980, Int. J. Control, 31, 109.

29. STEEB, W.H. and WILHELM, F., 1980, Journal of Math. Anal. & Applications, 77, 601.

30. RUGH, W.J., 1981, Nonlinear System Theory (Baltimore: The Johns Hopkins University Press).

31. KRENER, A., 1974, Proc. of the 1974 Allerton Conf., El. Eng. Dept., U. of Illinois, Urbana-Champaign, IL, 834.

32. BROCKETT, R., 1976, Functional Expansion and Higher Order Necessary Conditions in Optimal Control in Mathematical Systems Theory, Marchesini, G., Mitter, S., eds., Lecture Notes in Economics and Math. Systems, 131 (New York: Springer-Verlag).

33. TSILIGIANNIS, C.A. and LYBERATOS, G., 1987, Journal of Math. Anal. and Applications, 126.

34. LYBERATOS, G. and TSILIGIANNIS, C.A., 1987, Chem. Eng. Sci., 42.

35. TSILIGIANNIS, C.A. and LYBERATOS, G., 1987, Journal of Math. Anal. and Applications (in print).

36. PIPPARD, A.B., 1985, Response and Stability (Cambridge: University Press).

37. VERHULST, P.F., 1847, Nuox. Mem. Acad. Roy. Bruxelles, 18, 1.

38. MONOD, J., 1949, Ann. Rev. Microbiol. 3, 371.

39. TESSIER, G., 1936, Ann. Physiol. Physiocochium Biol., 12, 527.

40. MOSER, H., 1958, Carnegie Inst. Wash. Publ., 614.

41. WILLIAMS, F.M., 1967, J. Theoret. Biology, 15, 190.

42. JEFFERSON, C.D. and SMITH, J.M., 1973, Chem. Eng. Sci., 28, 629.

43. CHIAM, H.F. and HARRIS, J.J., 1982, Biotechnol. Bioeng., 24, 37.

44. BIJKERK, A.H.E. and HALL, R.J., 1977, Biotechnol. Bioeng., 19, 267.

45. BUSBY, J.B. and ANDREWS, J.F., 1975, J. Water Poll. Control Fed., 47, 1055.

46. PAMENT, N.B., HALL, R.J. and BARFORD, J.P., 1978, Biotechnol. Bioeng., 20, 349.

47. CHI, C.T. and HOWELL, C.T., 1976, Biotechnol. Bioeng., 18, 63.

48. AGAR, D.W. and BAILEY, J.E., 1981, Biotechnol. Bioeng., 23, 2217.

49. AIBA, S., HUMPHREY, A.E. and MILLIS, N.F., 1973, Biochemical Engineering (New York: Academic Press).

50. HUMPHREY, A.E., 1963, Proc. 5th Symposium, Inst. Appl. Microbiol., Univ. of Tokyo, 215.

51. SIKYTA, B., SLEZAK, J. and HEROLD, M., 1961, Appl. Microbiol., 9, 233.

52. MOO-YOUNG, M., 1975, Can. J. Chem. Eng., 53, 113.

53. BAILEY, J.E. and OLLIS, D., 1977, Biochemical Engineering Fundamentals (New York: McGraw-Hill).

54. CONTOIS, P.E., 1959, J. Gen. Microbiol., 21, 40.

55. GILLEY, J.W. and BUNGAY, H.R., 1968, Biotechnol. Bioeng., 10, 99.

56. WANG, N.S. and STEPHANOPOULOS, G.N., 1985, Biotechnol. Bioeng. Symposium Series, 113, 635.

57. SUNASTROM, D.W., KLEI, H.E. and BROOKMAN, G.T., 1976, Biotechnol. Bioeng., 18, 1.

58. LYBERATOS, G., 1985, Chem. Eng. Sci., 40, 2160.

59. BERENBAUM, M.C., 1969, Brit. J. Cancer, 24, 434-445.

60. VERHULST, P.F., 1847, Nuox. Mem. Acad. Roy. Bruxelles., 18, 1.

61. EISEN, M., 1979, Mathematical Models in Cell Biology and Cancer Chemotherapy (Berlin: Springer-Verlag).

62. GOMPERTZ, B., 1825, Phil. Trans. Roy. Soc. London., 115, 513.

63. BERTALANFFY, L., 1960, In W.W. Nowinsky (Ed.) Fundamental Aspects of Normal and Malignant Growth (Amsterdam: Elsevier), pp. 173.

64. SUMMERS, W.C., 1966, Growth, 30, 333

65. AYALA, F.J., 1973, Theor. Pop. Biol., 4, 331.

66. SALMON, S.E., and DUNE, B.G., 1977, In B. Drewinko and R.M. Humphrey (eds.) Growth Kinetic and Biochemical Regulation of Normal and Malignant Cells (Baltimore: Williams and Wilkins), pp. 815-877.

67. SIMPSON-HERREN, L., and LLOYD, H.H., 1970, Cancer Chemother. Rep. Part I., 54, 143-174.

68. SWAN, G.W., and VINCENT, T.L., 1977, Bull. Math. Biol., 39, 317-337.

69. ZIETZ, S., 1979, Cell Cycle Kinetic Modeling and Optimal Control Theory in the Service of Cancer Chemotherapy (Berkeley: Ph.D. Thesis).

70. COLLINS, J.M., and DEDRICK, R.L., 1982, In Pharmacologic Principles of Cancer Treatment. B. Chabner (ed.) (Philadelphia: Saunders).

BIOGRAPHICAL SKETCH

Eva-Maria Abulesz was born on September 10, 1958, to Eva-Maria and Karl Abulesz in Vienna, Austria.

She received her primary and secondary education in Vienna where she graduated from high school summa cum laude in 1976. She attended the Technical University of Vienna where she received the degree of Cand. Ing. in 1981 and the degree of Diplom-Ingenieur, summa cum laude, in 1982, both in technical chemistry.

After doing post-graduate work at the TU Vienna, she joined the University of Florida in 1983 on a Fulbright Scholarship and received her degree of Master of Science in 1984. While pursuing her education she has worked for numerous companies in Europe as well as the United Stated.

I certify that I have read this study and that in my opinion it conforms to acceptable standards of scholarly presentation and is fully adequate, in scope and quality, as a dissertation for the degree of Doctor of Philosophy.

Hong H. Lee, Chairman
Professor of Chemical Engineering

I certify that I have read this study and that in my opinion it conforms to acceptable standards of scholarly presentation and is fully adequate, in scope and quality, as a dissertation for the degree of Doctor of Philosophy.

Gerasimos K. Lyberatos, Cochairman
Assistant Professor of Chemical Engineering

I certify that I have read this study and that in my opinion it conforms to acceptable standards of scholarly presentation and is fully adequate, in scope and quality, as a dissertation for the degree of Doctor of Philosophy.

Spyros A. Svoronos
Associate Professor of Chemical Engineering

I certify that I have read this study and that in my opinion it conforms to acceptable standards of scholarly presentation and is fully adequate, in scope and quality, as a dissertation for the degree of Doctor of Philosophy.

Hartmut Derendorf,
Associate Professor of Pharmaceutics

I certify that I have read this study and that in my opinion it conforms to acceptable standards of scholarly presentation and is fully adequate, in scope and quality, as a dissertation for the degree of Doctor of Philosophy.

Gar B. Hoflund
Professor of Chemical Engineering

This dissertation was submitted to the Graduate Faculty of the College of Engineering and to the Graduate School and was accepted as partial fulfillment of the requirements for the degree of Doctor of Philosophy.

August 1988

Dean, College of Engineering

Dean, Graduate School